

# **Effect of intramolecular H-bonding and $\pi$ -stacking on the folding of periodically-grafted amphiphilic polyamides**

**Reena**

**MS16042**

*A dissertation submitted for the partial fulfillment  
Of BS-MS dual degree in Science.*



**Indian Institute of Science Education and Research, Mohali**

**April, 2021**

# Certificate of Examination

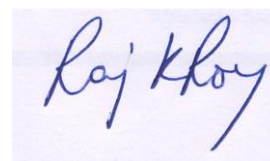
This is to certify that the dissertation titled “**Effect of intramolecular H-bonding and  $\pi$ -stacking on the folding of periodically-grafted amphiphilic polyamides.**” Submitted by Ms. Reena (Registration No. MS16042) for the partial fulfillment of the Indian Institute of Science Education and Research, Mohali's BS-MS dual degree programme has been examined by the thesis committee duly appointed by the Institute. The Committee finds the work done by the candidate satisfactory and recommends that the report be accepted.



Dr. Sugumar Venkataramani  
(Committee member)  
Assistant Professor  
IISER Mohali



Dr. Sanchita Sengupta  
(Committee member)  
Assistant Professor  
IISER Mohali




Dr. Raj Kumar Roy  
(Supervisor)  
Assistant Professor  
IISER Mohali

Date: April 30, 2021

# Declaration

I have carried out the work presented in this dissertation under the guidance of Dr. Raj Kumar Roy at the Indian Institute of Science Education and Research Mohali. This work has not been submitted in part or in full for a degree, a diploma, or a fellowship to any other university or Institute. Whenever contributions of others are involved, every effort is made to indicate this clearly, with due acknowledgment of collaborative research and discussions. This thesis is a bonafide record of original work done by me, and all sources listed within have been detailed in the bibliography.

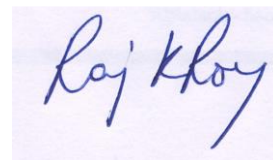


Reena

(Candidate)

Date: April 30, 2021

In my capacity as the supervisor of the candidate's project work, I certify that the above statements by the candidate are true to the best of my knowledge.



Dr. Raj Kumar Roy  
(Supervisor)

# Acknowledgment

I would like to thank my esteemed supervisor, Dr. Raj Kumar Roy, Assistant Professor, Department of Chemical Sciences, Indian Institute of Science Education and Research Mohali, for giving me the opportunity to undertake my MS thesis project under your research group. Many thanks for his invaluable guidance, encouragement, support, and help to complete this project. During the project, he helped me with critical intellectual feedback when I needed it the most.

I express my sincere gratitude and most respectful regards to my committee members Dr. Sugumar Venkataramani and Dr. Sanchita Sengupta, for their valuable suggestions, guidance, and comments during presentations.

I am extremely grateful to thank Mr. Subendhu Samanta, for his continuous support, advice, and guidance during experimental work. His immense knowledge and a lot of experience helped me a lot during my academic research.

A lot of thanks to my grandfather Mr. Jagram Yadav, my parents, and my whole family for their immense love, care, support, motivation, trust, and for everything they have given to me. I'm so blessed to have each of them in my life. Thank you for everything!

I would also like to thank my friends Susmita, Anjali Gupta, Neha Bajaj, Vishal Tiwari, Rahul Singh Yadav, Deepraj, Gaurav, Yuvraj, Sukram, and Devanshu for their help, motivation, and late-night talks.

I am especially grateful for very generous additional help from my lab group members Deepak, Ankita, Arjun, and Umer for their love, care, and support. Working in the RKR group with such kind and humble people has been a great experience. Thanks for being there for me.

I would also like to thank SSG group members Narendra Tripathi, Sushil, Anita, Kavita, Roshmi, Kirti for their help and support.

# Contents

List of figures.....	1
List of Schemes.....	3
List of abbreviations.....	4
Abstract.....	5
Chapter 1 Introduction.....	6
Chapter 2 Result and Discussions.....	21
Chapter 3 Summary and Outlook.....	33
Chapter 4 Experimental section.....	35
References.....	47
Appendix.....	51

# List of figures

**Figure 1:** Static oligomers that adapt a well-defined conformation without folding reaction. a) Helicenes, b) oligonaphthalenes, c) polyprolines, and d) polyisocyanates

**Figure 2:** Helix-coil transition model: Initiation of helical folding, followed by propagation steps to form a helix from the coil.

**Figure 3:** Molecular structure of folded conformation due to donor-acceptor charge transfer complex.

**Figure 4:** A Quinoline foldamer.

**Figure 5:** a.) Structure of molecular strand (intramolecular hydrogen bonds leads to the folding.) b.) Helical structure of the above molecular strand.

**Figure 6:** a.) Structure of heptameric molecular strand. b.) Cyanurate template. c.) Stabilization after binding to the template.

**Figure 7:** (a) Molecular strand stabilized by both intramolecular hydrogen bonding and  $\pi$ - $\pi$  stacking. (b) Molecular strand stabilized by  $\pi$ - $\pi$  stacking

**Figure 8:** Structure of target **POLY 11** assisted by intramolecular hydrogen bonding.

**Figure 9:** Structure of target polymer **POLY 10**.

**Figure 10:** Structure of **POLY 11** after post-polymer modification.

**Figure 11:**  $^1\text{H}$  NMR spectra of **POLY 11** and **POLY 10** in DMSO.

**Figure 12:**  $^1\text{H}$  NMR of **POLY11** and **POLY 10** after CuAAc Click reaction in DMSO.

**Figure 13:** Absorption spectra of **POLY 10(PEG 550)** and **POLY 11(PEG550)** in TCE. Inset: The variation of absorbance vs. concentration follows Beer-Lamberts law.

**Figure 14:** Absorption spectra of polymers **POLY 10(PEG 550)** and **POLY 11(PEG 550)** in DMSO. Inset: Calibration curve follows Beer-Lambert law.

**Figure 15: POLY11 (PEG550) and POLY 10 (PEG 550) on the addition of TFA.**

**Figure 16: Absorption spectra of POLY10 (PEG550) and POLY11 (PEG550) in different DMSO and water ratios.**

**Figure 17: Absorption of Host-guest complexation of POLY 10 (PEG550) and POLY11 (PEG550) with Maleimide.**

# List of Schemes

**Scheme 1:** General synthesis scheme for **monomers A and B**

**Scheme 2:** Synthesis scheme for the preparation of **POLY 10** and **POLY 11**.



# List of Abbreviations

$^1\text{H-NMR}$	Proton NMR
$\text{CDCl}_3$	Deuterated chloroform
$\text{CHCl}_3$	Chloroform
DCM	Dichloromethane
DMF	Dimethylformamide
DMSO	Dimethylsulphoxide
HMPA	hexamethylphosphoramide
$\text{K}_2\text{CO}_3$	Potassium Carbonate
$\text{Na}_2\text{SO}_4$	Sodium Sulphate
$\text{NaHCO}_3$	Sodium Bicarbonate
nm	Nanometer
NMP	N-Methyl-2-Pyrrolidone
NMR	Nuclear magnetic resonance
RT	Room Temperature
TCE	1,1,2,2 Tetrachloroethane
THF	Tetrahydrofuran
UV-Vis	Ultraviolet Visible

# Abstract

The study of natural biological systems where covalent and non-covalent molecular interactions between unique units in their sequence aid folding into a well-defined three-dimensional structure inspired the field of foldamer chemistry. In this work, two different aromatic oligoamide foldamers were synthesized and characterized by  $^1\text{H}$  NMR, UV-Visible spectroscopy. The plan was to synthesize  $\pi$ -electron rich foldamers in which conformational preferences can be induced through different covalent and non-covalent interactions (for example, hydrogen bonding). The target polymer **POLY 11** consists of donor group 1, 5-diaminonaphthalene, and monomer hydroxyl substituted chelidamic acid, i.e., a potential candidate to facilitate intramolecular hydrogen bonding; predicted that this would induce a random coil structure into a well-organized foldameric system. All of the backbone's structural features are designed to aid in the folding process. The primary outcome of work is after post-polymerization modification that helps in solubility of the polymer in different organic solvents. Conclusions regarding stable folded conformations along the polymer chain were inferred from NMR and UV-Vis spectroscopy.

# Chapter 1

## Introduction

Despite the small number of amino acids they are composed of, proteins perform a wide range of roles within nature. In biological chemistry, a well-established theory is that the structure and conformation of large, complex biomolecules are crucial to perform a function. The vast range of chemical functions emerging from biopolymers has inspired chemists to design synthetic systems that can mimic these elegant long-chain molecules' structural and functional features<sup>1</sup>. Chemists have a huge opportunity to learn and adapt biological molecules for chemical applications because of their extensive abilities. While attempts to mimic molecular recognition, catalysis, and other functions have resulted in the creation of molecular-imprint polymers<sup>2</sup>. The attempt to understand these structural features and mimic the biological system gives rise to the area of foldamers<sup>5</sup>. The motivation behind this is to generate spatially well-organized complex structures by direct folding through covalent and non-covalent interactions. The desire to emulate the elegance of nature while at the same time expecting that this would allow bridging the gap between the molecular and macroscopic scale in terms of structural evolution<sup>3</sup>.

### 1.1 Foldamers

#### 1.1.1 Definition and Background

S.H Gellman was the first to introduce the term foldamer in 1996. There has been a various definition of foldamers, but the most detailed definition is outlined by J.S Moore *et al.* where they described the foldamer as "*any oligomer that folds into a conformationally ordered state in solution, the structure of which is stabilized by the collection of non-covalent interactions between non-adjacent monomer units.*"<sup>4</sup> These molecules are designed to mimic biopolymer's structure and interactions and to fold into well-defined conformations<sup>5</sup>. It is well known that the functioning of biomolecules is controlled by conformation. But the control of polymer conformations in solution is extremely challenging. Conformational control is

achieved through several intramolecular non-covalent interactions that provide enthalpic contribution to overcome the folding process's entropic barrier. The critical concern in foldamer science is how the primary oligomeric sequence folds into conformationally ordered structures and how individual subunits self-associate into assemblies. According to the term foldamers description, one main criterion is a dynamic conformation needed to classify an oligomer as a foldamer. Therefore, static oligomers with pre-determined conformations, or oligomers with well-ordered conformations through their torsional potential energy surface, are not considered foldamers. Examples include Helicenes<sup>6,7</sup>, oligonaphthalenes<sup>8</sup>, polyisocyanates<sup>9</sup>, polyprolines<sup>10</sup>, and polyaldehydes<sup>11</sup>.

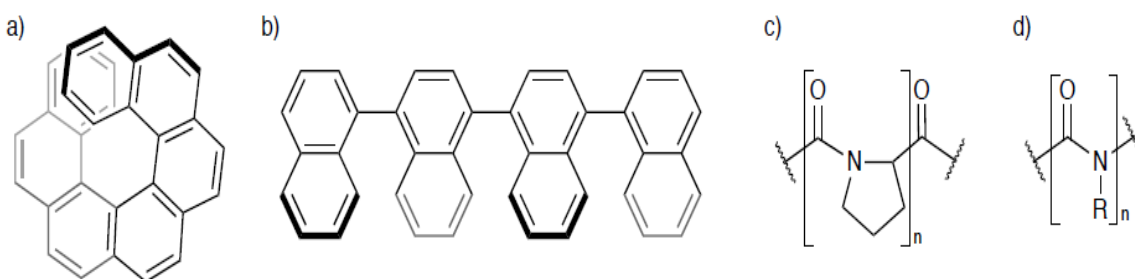


**Figure 1:** Static oligomers that adapt a well-defined conformation without folding reaction. a) Helicenes, b) oligonaphthalenes, c) polyprolines, and d) polyisocyanates.<sup>4</sup>

### 1.1.2 Thermodynamics of folding

When designing a molecular structure to adopt a folded conformation, it is necessary to consider the thermodynamic and kinetic parameters involved in the folding process. To continue folding, the process must be energetically favorable. When folding occurs, there is a loss in entropy due to decrease in randomness. Therefore, the resulting conformation has to compensate for the loss in entropy by the gain in enthalpy through structurally stabilizing non-covalent interactions.

## Folding of Helices

This can be explained by using statistical thermodynamics to describe the transition from higher energy unfolded state to stable lower energy folded conformation. Zimm and Bragg first described this as a one-dimensional problem<sup>12</sup>. This includes cooperative-phase transitions and can be described in terms of the nucleation/propagation model<sup>13</sup>. Initially, when an oligomeric chain starts to fold into a helix structure, there is a loss of entropy without energy gain; this is called nucleation of helix formation. Once this coil to helix nucleation has occurred, there will be a loss of conformational entropy and gain in energy on each conversion step. This net energy gain results from interaction energy of stabilizing non-adjacent monomers' interactions, which can only be achieved after the initiation of helix formation. This stage of coil to helix transition is called 'propagation.' Initially, helical folding is unfavorable due to loss in entropy until it reaches a chain length at which the enthalpic gain of interaction surpasses that loss, followed by cooperative transition when the change in free energy between coil and helix becomes negative at the folding temperature<sup>4</sup>.

Kinetic parameters are generally negligible when we design a helical foldamer. Helices have been experimentally shown to fold on a time scale of milli-to microseconds<sup>14</sup>. Folding is so fast enough that any small structural change to the chain doesn't make any significant difference to the rate of folding as long as the thermodynamic propensity of small helices to fold is retained<sup>4</sup>. Therefore, thermodynamic parameters, conformational entropy, and the overall energetic difference between unfolded and folded oligomeric chains are the primary concern to achieve foldameric properties<sup>4</sup>.

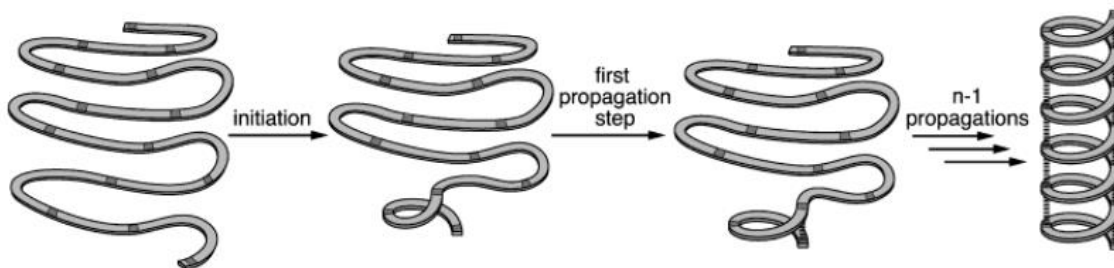


**Figure 2:** Helix-coil transition model: Initiation of helical folding, followed by propagation steps to form a helix from the coil.<sup>4</sup>

Both internal and external factors have significant influences on the folding of helices and foldamers. The internal factors to be considered are rigidity of the backbone, configuration of the molecule, non-covalent interactions to stabilize its conformation, type of linkage between its monomers, and orientation. External factors to be considered for the process of folding are solvent-dependent hydrophobic effects, host-guest complexation.

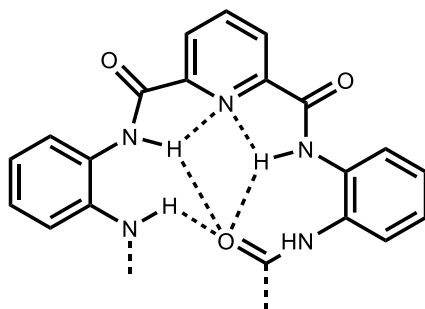
### 1.1.3 Folding interactions

The main features of folding in foldamers like change in conformation, ability to unfold, and continuity of effect of the folding motif in long-chain molecules or the consequences which allow the formation of stable oligomeric structures. This is achieved through various non-covalent interactions. Hydrogen-bonding<sup>15</sup> is the most common among them, further supported by  $\pi$ - $\pi$  interaction, metal-ion coordination<sup>16</sup>, host-guest interaction<sup>17</sup>, charge-transfer complexation<sup>18</sup>, and solvophobic effect<sup>19</sup>. Some of them are discussed in the following section.

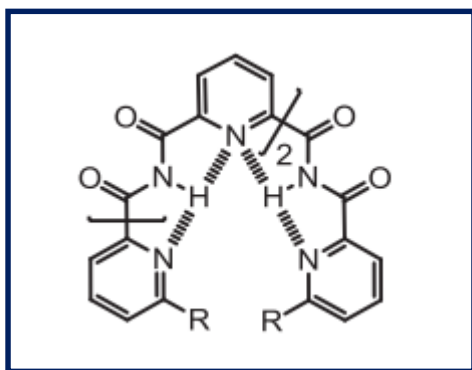
**Hydrogen-bonding:** While hydrogen bonds are not as stable and rigid as covalent bonds, their directionality, stabilizing power, and ability to organize molecules in a solution state cannot be overstated. The folding of oligomers is firmly guided by the directionality and stability of hydrogen bonds.

The amide bond is the most common hydrogen bonding group used in foldamer design. Since the amide bond has both a donor and an acceptor group, it can be used to build a hydrogen bond network in foldamers<sup>20</sup>. The partial double bond character of the carbonyl group's nitrogen and carbon atoms makes it rigid, brings planarity, and creates a significant energy barrier for bond flipping which stabilizes the folded structure.

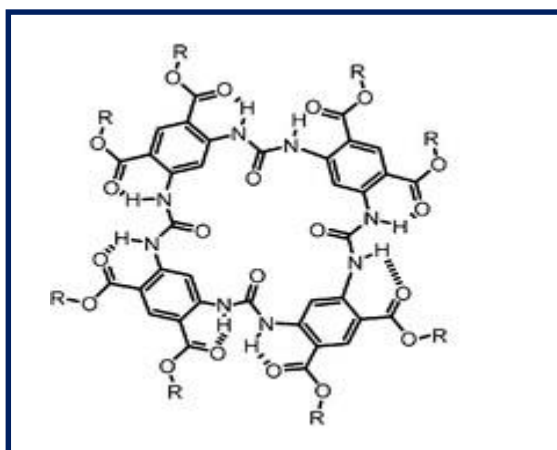
In 1994 Hamilton et al. were the first to discover the series of secondary helical structures of aromatic amide oligomers stabilized by an intramolecular three-centered hydrogen bonding network. Zhang and coworkers developed a series of foldamers that consists of benzene and pyridine segments<sup>21</sup>. The selected backbone, as shown in the structure below, is relatively short and produces no cavity.



The backbones other than the amide-derived backbone have also led to considerable success.



(a)



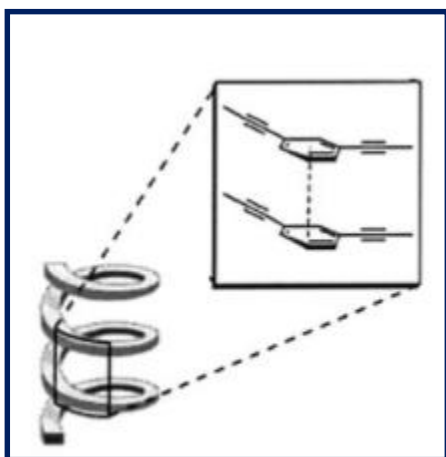
(b)

a.) Zhan and Yao, and coworkers reported that imide-pyridine-linked oligomers were forced to show helical conformation of large curvature due to N-H---N intramolecular hydrogen bonding<sup>21</sup>.

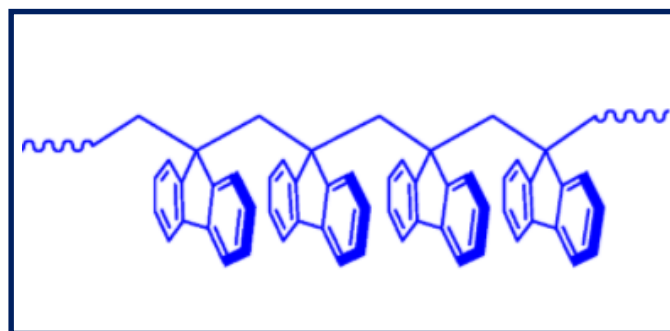
.

b.) Gong and group reported aromatic oligoureas composed of aromatic rings and connected through the urea functionalities. In this case, also intramolecular hydrogen bonding enforces the process of folding<sup>22</sup>.

**$\pi$ - $\pi$  Stacking:** In the 1990s, Hunters and Sanders were the first to propose a model that predicts aromatic stacking geometry that centered on the overall polarization of aromatic  $\pi$ -electron cloud<sup>23</sup>. Molecules can be assembled in various ways among them; one is the  $\pi$ -stacked assembly in which planar aromatic molecules align closely in a parallel, cofacial manner. The assemblance of molecules due to  $\pi$ -stacking often shows characteristic physical properties like excimer formation on photoexcitation and charge transport. For example,



(a)



(b)

a.) Oligomeric m-phenylene ethylenes are stabilized by  $\pi$ -stacking interactions of similar nature aromatic rings. Here the driving force for folding is  $\pi$ - $\pi$  interaction and solvophobic interaction in polar solvents<sup>24</sup>.

b.) Poly dibenzofulvene (poly DBF) is an example of a  $\pi$ -stacked stabilized polymer. In poly (DBF), the side-chain aromatic groups are tightly stacked on top of each other along the almost all-trans main chain<sup>25</sup>.

**Solvophobic effects:** Aromatic interactions are strongly solvent-dependent. The utilization of the solvophobic effect requires the proper positioning of both hydrophobic and hydrophilic groups to ensure foldamer design folding. In weakly



interacting solvents (non-polar), the electrostatic force between electron-rich and electron-deficient groups dominates, while in strongly interacting solvents (polar), the solvophobic effect dominates over the other. So, the stacking of aromatic molecules in solutions is according to the dominant among both electrostatic and solvophobic effect, which will ensure the folding process<sup>26</sup>.

**Donor-Acceptor charge transfer mediated folding:** Various foldamers exploit interactions between aromatic units to drive their assembly into a predictable fashion. Here, they describe the synthesis of molecules that fold into a pleated structure due to interaction between electron-rich unit DAN (1, 5-dialkoxynaphthalene) and electron-deficient NDI (1, 4, 5, 8-naphthalene tetracarboxylic diimide) in solution. These aromatic units are linked together with a flexible peptide linker. As depicted in figure 3, they used glutamic acid residues to impart water solubility. Prevent aggregation. Along with that, folding is also assisted with solvophobic interaction in the water<sup>18</sup>.

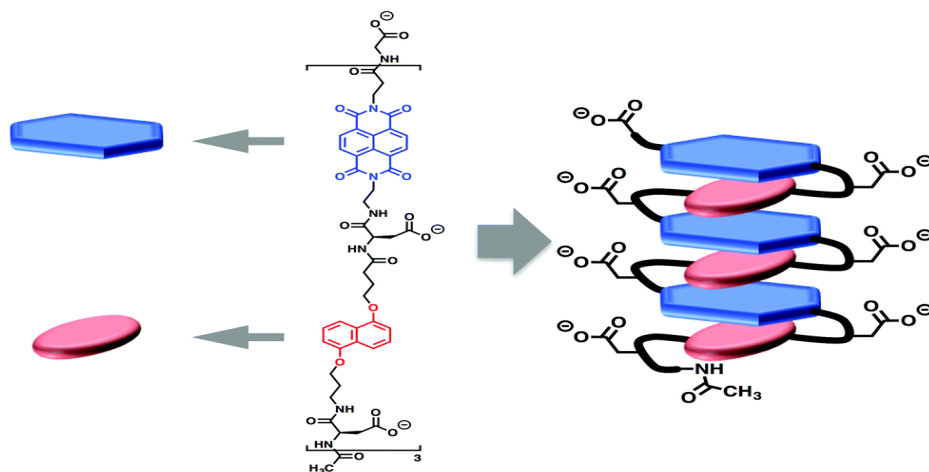


**Figure 3:** Molecular structure of folded conformation due to donor-acceptor charge transfer complex<sup>26</sup>.

### 1.1.4 Foldamer secondary structure

Foldamer's secondary structure follows the same rules as that of protein's secondary structure. The helix is the most important secondary folding motif in both proteins and foldamers. The chirality of the molecule will determine whether a helix will be right-handed or left-handed. The secondary structural propensity (SSP) of an amino acid is the significant determinant of protein conformation. The structure of each monomer creates a thermodynamic driving force that causes it to occupy a specific secondary structural environment<sup>27</sup>. One method for controlling conformation is to take advantage of non-covalent interactions between adjacent monomers.

### 1.1.5 Aromatic oligoamide foldamers

Aromatic oligoamide foldamers are a versatile class of synthetic oligomers that adapt highly stable and predictable folded conformations in a solution as a result of stabilizing intramolecular interactions between adjacent monomer units<sup>28</sup>. For example, Huc et al. have extensively investigated quinoline-based foldamers and quinoline-pyridine foldamers. Intramolecular hydrogen bonding between the amide hydrogen and adjacent quinoline nitrogens is expected to stabilize a bent shape, eventually giving rise to a helix for strands as short as a trimer<sup>29</sup>. By placing the amide bond's substitutes at a roughly 60° angle to each other, the quinoline unit was designed to produce relatively sharp turns in the helical structure, as depicted in figure 4. This enables efficient folding without the use of turn units. The amide bonds face the inside of the molecule, shielding it from solvent molecules and filling the molecular fold's inner part.

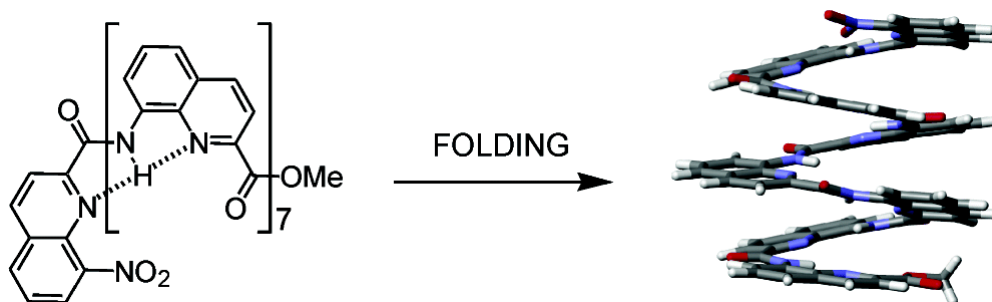
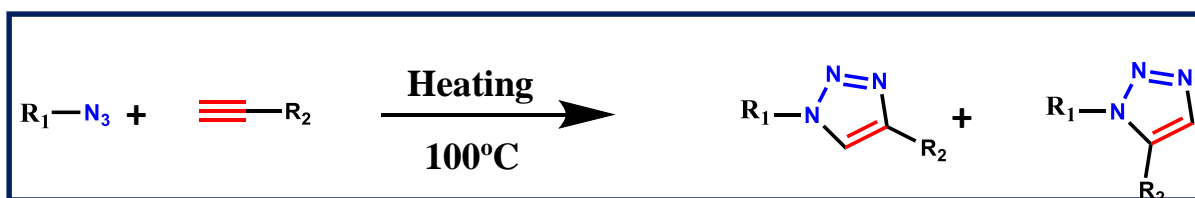


**Figure 4:** A Quinoline foldamer<sup>29</sup>.

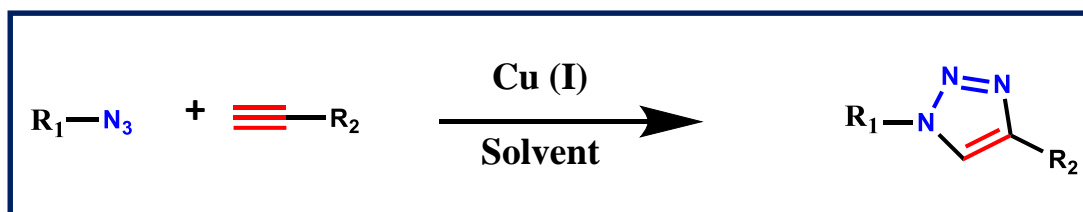
## 1.2 Copper-catalyzed azide-alkyne cycloaddition (CuAAC)

### Click reaction:

Before the Copper being used in the reaction, Huisgen and coworkers studied azide-alkyne cycloaddition. Huisgen cycloaddition refers to the non-catalyzed cycloaddition reaction between azide and alkyne to produce a 5-membered triazole ring. This kind of reaction's major drawbacks is the lack of selectivity between 1, 4, and 1, 5-disubstituted 1, 2, 3-triazole regioisomer being formed, high reaction temperature, and slower kinetics. K. Barry Sharpless and Meldal introduce the concept of Copper-catalyzed azide-alkyne cycloaddition click reaction in 2001. Using Copper as a catalyst for this reaction solved the problems described above associated with these reactions. The reaction proceeds at a faster rate and an ambient temperature by using Copper as a catalyst with complete conversion to the 1,4-disubstituted 1,2,3-triazole product<sup>30,31</sup>.



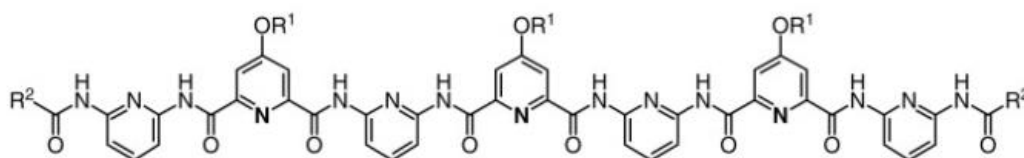
Huisgen cycloaddition



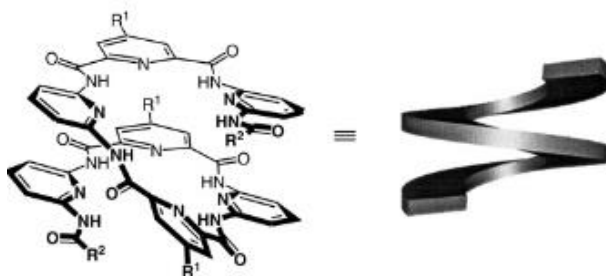
Copper-catalyzed azide-alkyne cycloaddition (CuAAC)

### 1.3 Motivation and Objectives:

This project's motivation is from the reported 2, 6 pyridine oligoamide foldamers in which folding is mainly directed by intramolecular hydrogen bonding between consecutive units along with a weak  $\pi$ -stacking interaction between two distant aromatic units (i & i+3)<sup>32</sup>. They have synthesized an oligomeric molecular strand composed of alternating 2, 6 diaminopyridine, and 2, 6 pyridinedicarbonyl units. These are designed such that they self-organize themselves into single-stranded helical structures by utilizing the non-covalent interactions mentioned previously<sup>32,33</sup>. As depicted in figure 5, the nitrogen atom present in the 2, 6 dicarboxamide series is expected to engage in an extended intramolecular hydrogen bonding with neighboring amide hydrogens throughout the oligomeric strand. So, the presence of such extensive intramolecular hydrogen bonding interactions within a single chain stabilized those oligoamides into a well-defined helical conformation.



(a)



(b)

**Figure 5:** a.) Structure of molecular strand (intramolecular hydrogen bonds leads to the folding) b.) Helical structure of above molecular strand<sup>32</sup>.

In a similar study from the same group, the alternate 2, 6 pyridinedicarbonyl was replaced by isophthalic acids such that the extensive H-bonding within the

oligomeric strand was no longer available (Figure 6). In such a situation, carbonyl bonds have a low energy barrier, so rotation around this occurs and leads to different rotamers formation, and hence conformation control was not achieved. Interestingly, a well-defined secondary structure was accomplished by introducing cyanurate as a template wherein the pyridyl amide moieties of the oligomeric backbone engaged into a six-point H-bonding with the external cyanurate derivatives<sup>32,34</sup> as shown in Figure 6.

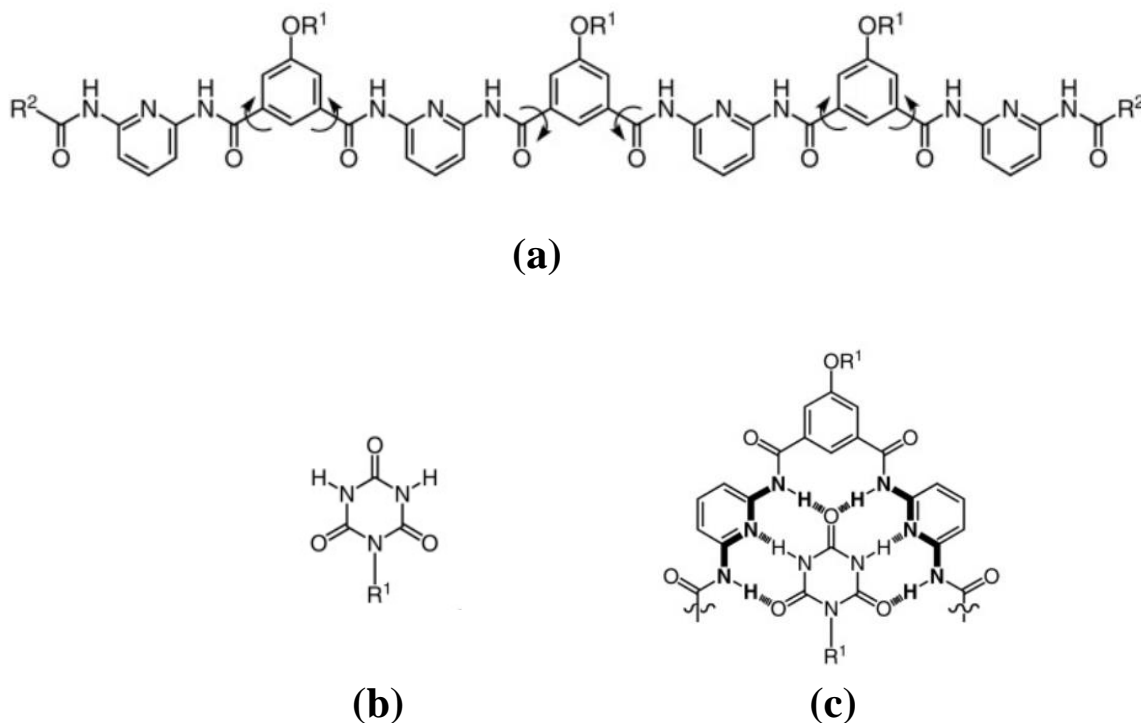


**Figure 6:** a) Structure of heptameric molecular strand. b) Cyanurate template. c) Stabilization after binding to the template<sup>32,34</sup>.

In an extension of the previous work, we have replaced isophthalic units with  $\pi$  electron-rich naphthalene units such that  $\pi$ -stacking interaction plays an important role in stabilizing the conformation-controlled folded structure without the use of any external template. In order to understand the role of intramolecular H-bonding on the folded configuration, we have prepared another polymer that cannot form any intramolecular H-bonding, as shown in Figure 7.

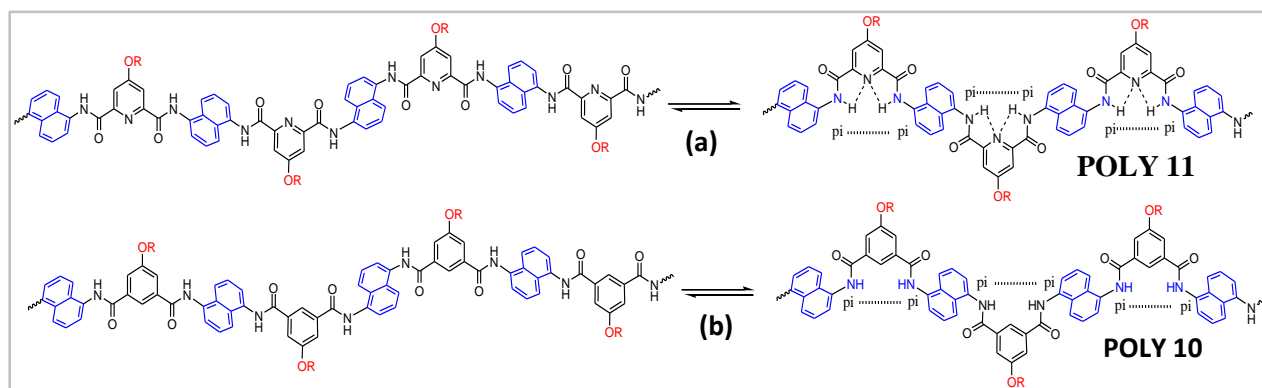


**Figure 7:** (a) Molecular strand stabilized by both intramolecular hydrogen bonding and  $\pi$ - $\pi$  stacking (**POLY 11**). (b) Molecular strand stabilized by  $\pi$ - $\pi$  stacking (**POLY 10**).

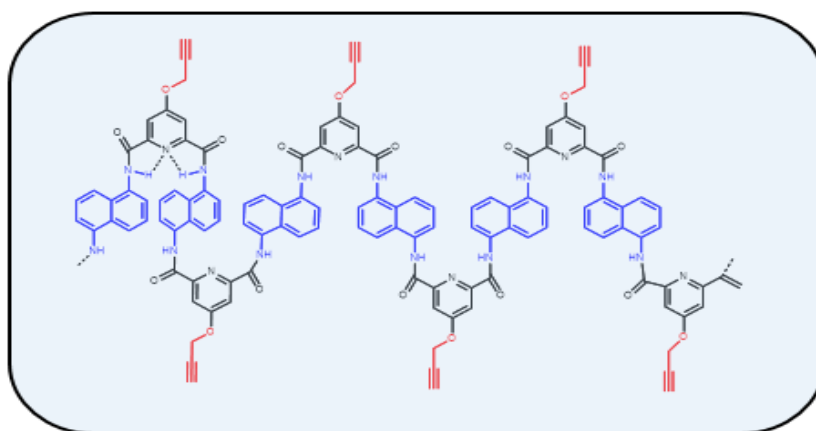
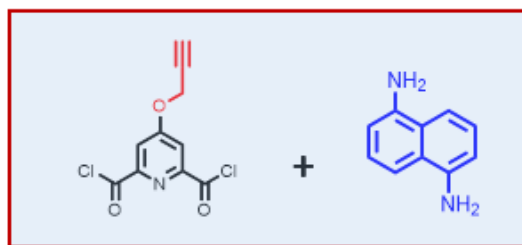
As mentioned earlier, Huc *et al.* group reported the oligopyridine-dicarboxamide based foldamers; it was synthesized by using a stepwise approach method employing monomers 2, 6-diaminopyridine, and 2, 6-pyridinedicarboxyl with substitution at the 4<sup>th</sup> position to enhance the solubility of these compounds in common organic solvents. Based on the research outlined in section 1.3, this project focuses on creating two different types of aromatic oligoamide foldamers, varying the extent of non-covalent interactions and their cooperativity to explore and exert conformational control. As shown in Figure 7, among the two possible conformations of amide units in equilibrium, it was anticipated **Poly 11** would stabilize in the folded conformation (right side) due to the cooperative non-covalent interactions as  $\pi$ -stacking and H-bonding. In order to test our hypothesis, I have used UV-Visible and NMR spectroscopy as a tool to monitor the folding propensity of these polymers at various solvents. Mainly, we are interested in knowing whether previously mentioned non-covalent interactions work in a cooperative manner to stabilize the folded structure or pose an orthogonal relationship to each other. For example, does the intramolecular H-bonding enhance the  $\pi$ -stacking interactions between naphthalene units? Similarly, does the  $\pi$ -stacking interactions between naphthalene units automatically lead to better intramolecular H-bonded structure?

## 1.4 Design of the folded structure:

This work aims to synthesize and analyze two polymer's folding behavior that differs in constituent monomer units. Here we choose  $\pi$  electron-rich 1, 5-diaminonaphthalene in both the polymers and hydroxyl-substituted chelidamic acid as a linker. The isophthalic one is analogues of this as a linker to compare these two polymer's folding propensity. Both linkers are substituted with the Propargyl group, thereby giving a reactive handle for post-polymerization modification to improve the polymer's solubility.

We predict that **POLY 10** (comprising 1, 5 diaminonaphthalene and substituted isophthalic unit) will prefer to stay in an entropy-driven less-folded structure. While introducing another monomer unit in the system, conformational changes can occur predictably. The predicted conformation is adapted in the target polymer due to the driving force intramolecular hydrogen-bonding between the amide and substituted monomer moiety (figure 8), i.e., **POLY 11** (comprises 1, 5 diaminonaphthalene and hydroxyl-substituted chelidamic unit).

### Monomer unit



Repeat  
unit

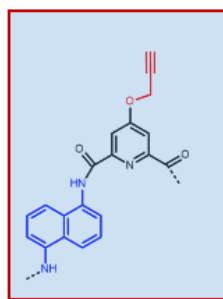


**Figure 8:** Structure of target **POLY 11** assisted by intramolecular hydrogen bonding.

To compare the folding properties of POLY 11, we synthesized an analogous polymer **POLY 10**.

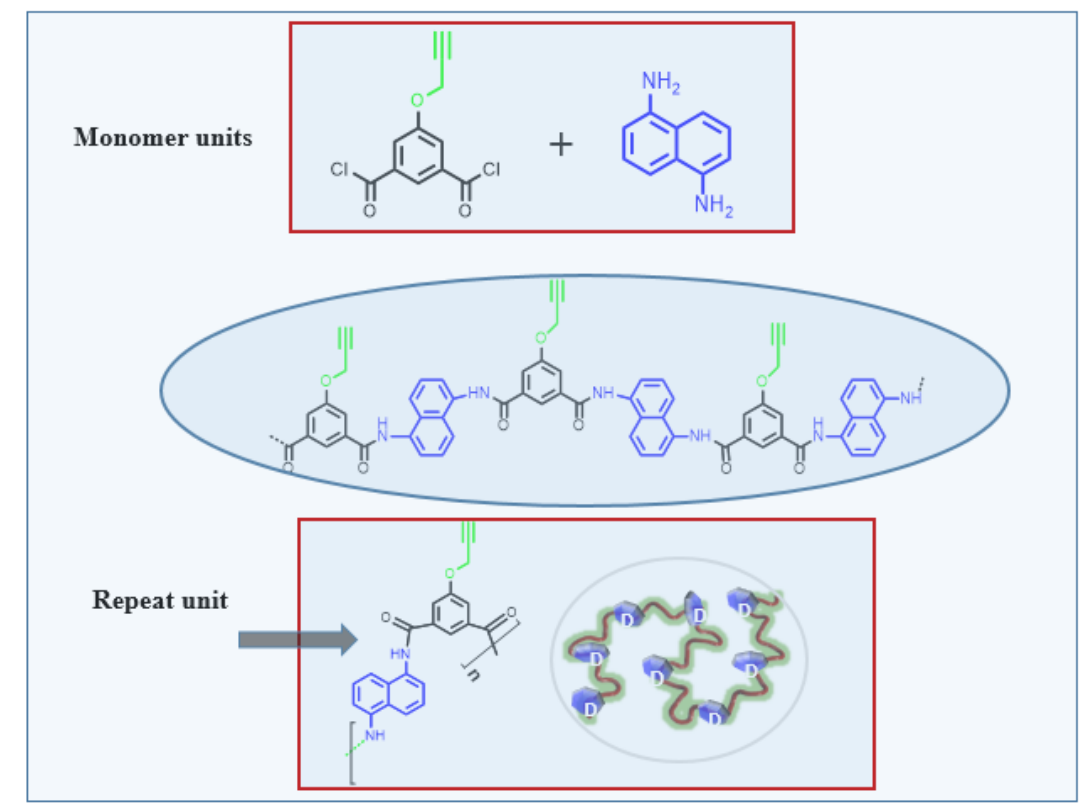


**Figure 9:** Structure of target polymer **POLY 10**.



Post-polymerization modification was done at the Propargyl group, acting as a reactive handle. CuAAC is a very promising click reaction between an azide and terminal alkynes. Modification at the polymer's molecular structure is typically done to give the manufactured material better properties like reactivity, thermal stability, and solubility, etc. We anticipated that such modifications would render the polymer to soluble in common organic solvents such that folding studies can be done in various solvents, including in water.

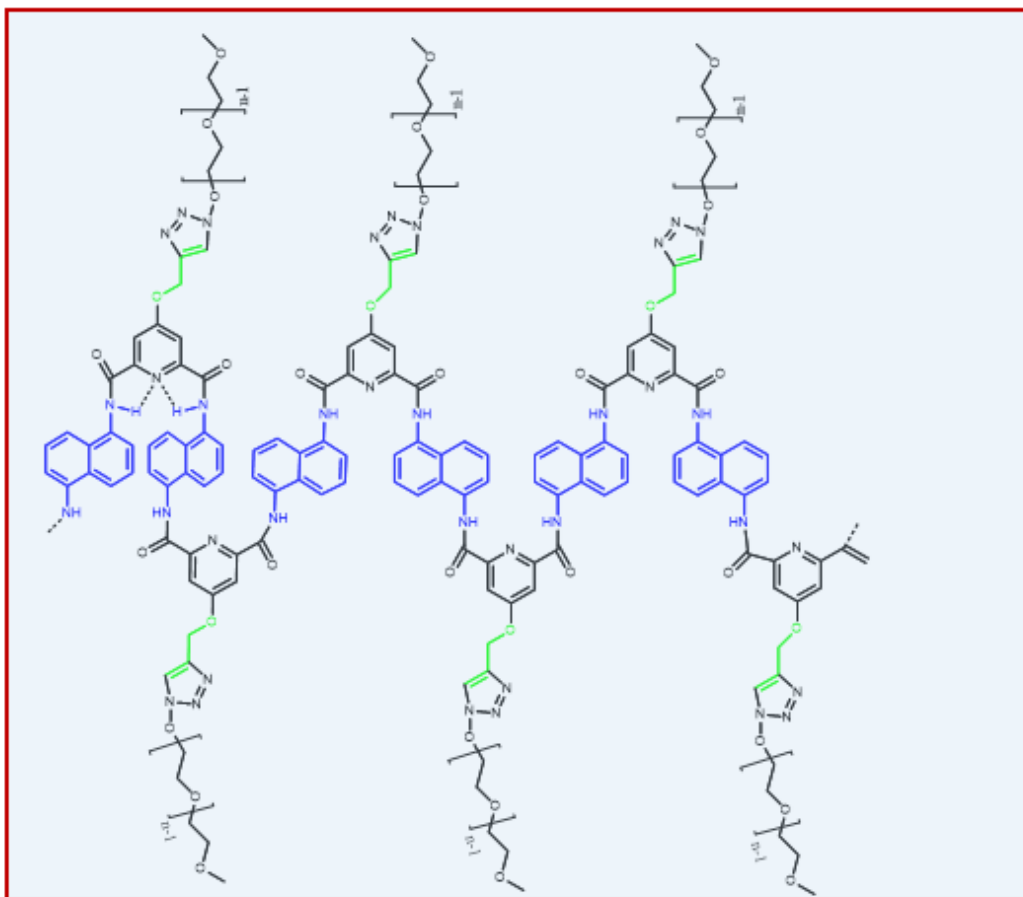


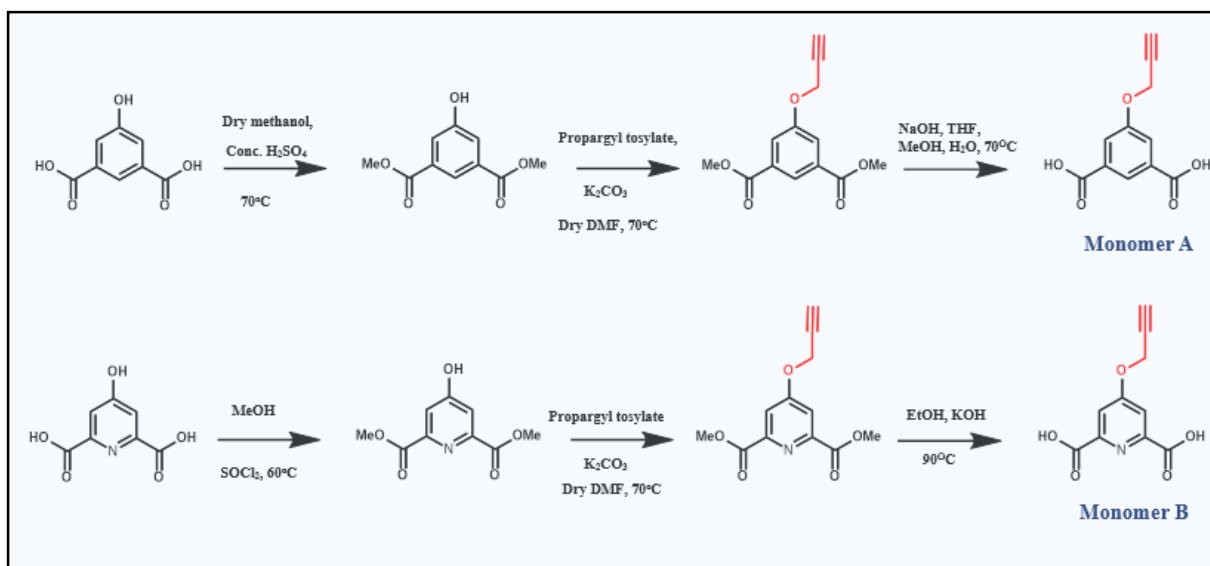
**Figure 10:** Structure of **POLY 11** after post-polymer modification.

# Chapter 2

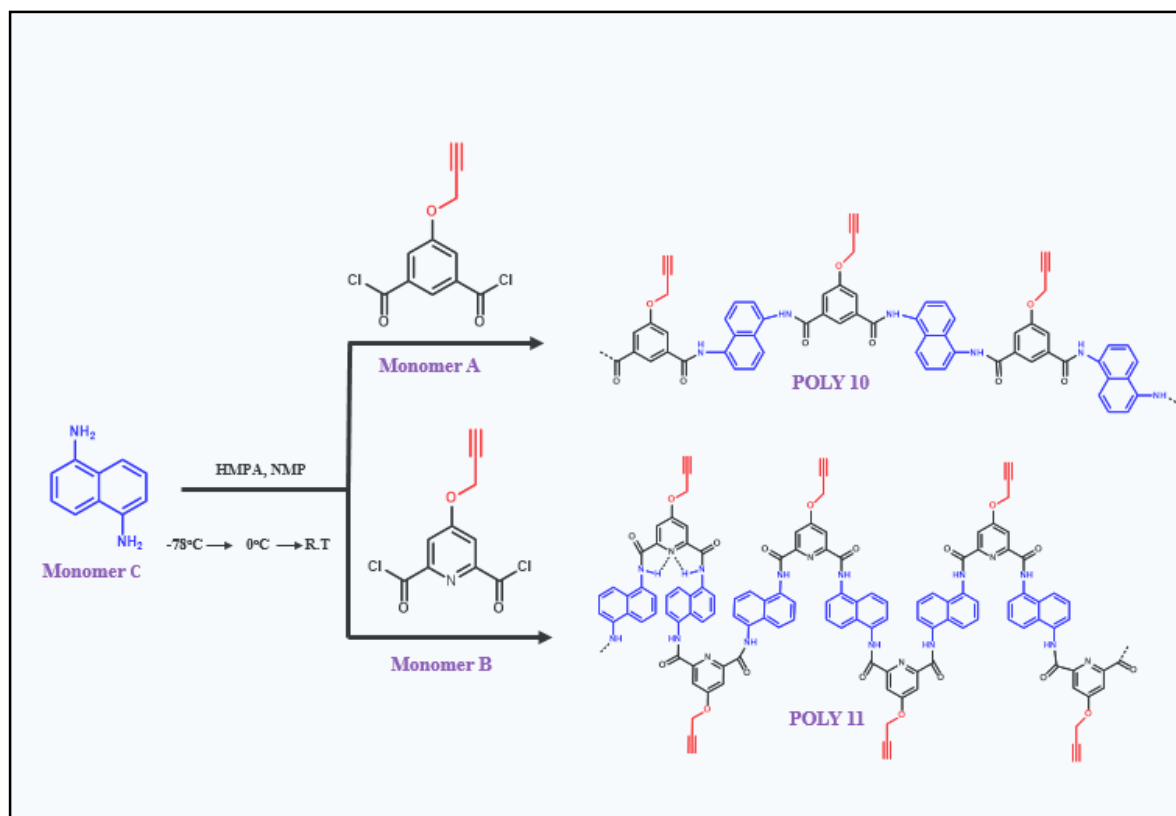
## Results and discussion

### 2.1 Synthesis

We commenced our project with the aim of synthesizing monomer candidates to yield two different polymers with different folding behavior. The **POLY 10** and **POLY 11** have been considered as the target polymer for comparing these two polymer's folding propensity in this thesis. In this regard, two **monomers A and B**, with different intrinsic properties, have been synthesized as shown in scheme 1 to prepare **POLY 10** and **POLY 11**, respectively.



**Scheme 1:** General synthesis scheme for **monomers A and B**

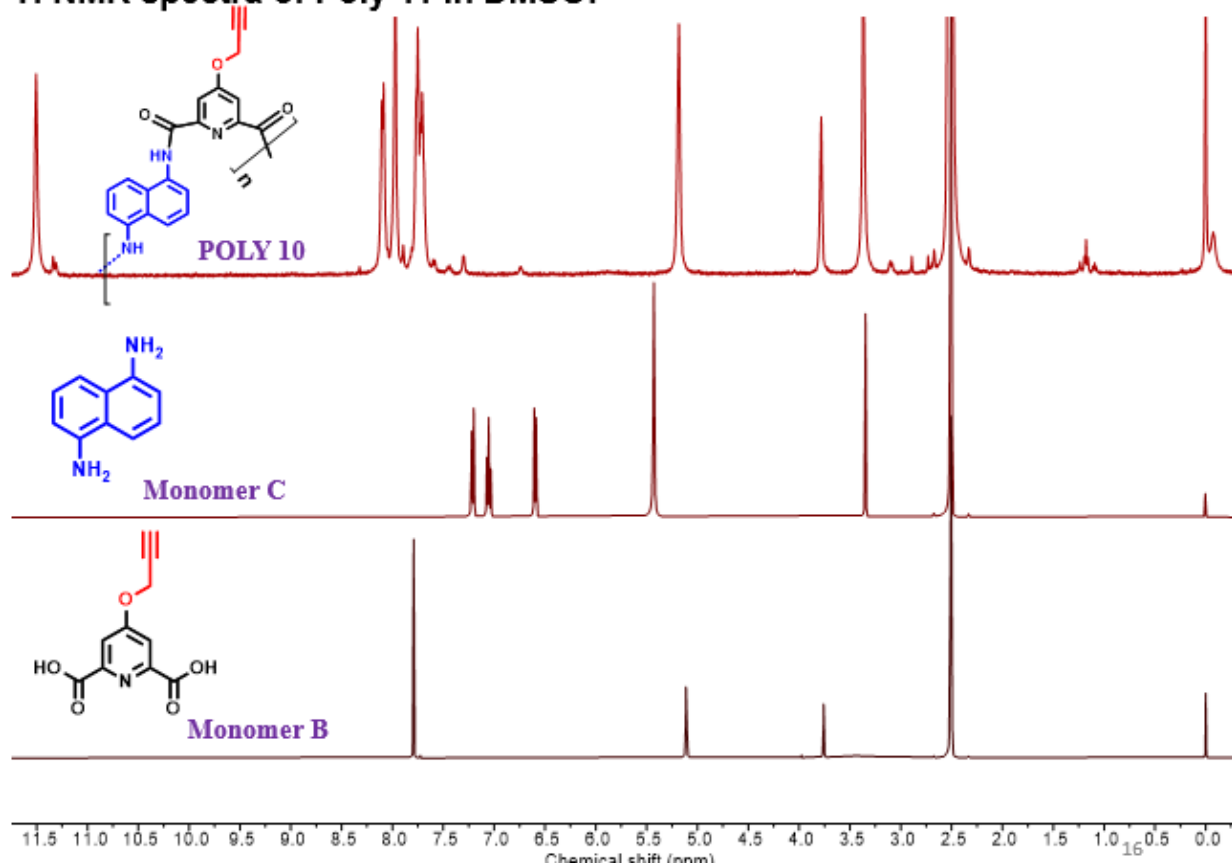


**Scheme 2:** Synthesis scheme for the preparation of **POLY 10** and **POLY 11**.

Finally, the target polymers were synthesized, as shown in the scheme. Herein, DMSO is not used as a solvent because oxalyl chloride and DMSO can give side reactions like swern oxidation. To avoid the side reaction, HMPA (hexamethylphosphoramide) and NMP (N-Methyl-2-Pyrrolidone) are used as a solvent, as these are well-known solvents for dissolving polyamides. These solvents are highly basic in nature to neutralize the formed HCl in the reaction to attain the equilibrium between the monomer and the polymer units in the forward direction. The polymer's solubility was tested and found to be insoluble in most of the common organic solvent systems except DMSO. The low molecular weight polymers were then removed from the system by continuous precipitation from the DMSO by adding solvent chloroform. Figure 11 (a) depicts the  $^1\text{H}$  NMR spectra of **POLY 11** with the characteristic signal of amide protons 11.5 ppm. The aromatic region of 1, 5 diaminonaphthalene and **monomer B** shows peaks in the range of 7.5-8.6 ppm. The peaks at 5.2 ppm and 3.6 ppm correspond to the methylene ( $-\text{CH}_2$ ) group and terminal hydrogen ( $-\text{CH}$ ) of propargylic group protons. Figure 11 (b) depicts the  $^1\text{H}$  NMR spectrum of **POLY 10** with the characteristic signal of amide protons at 10.5

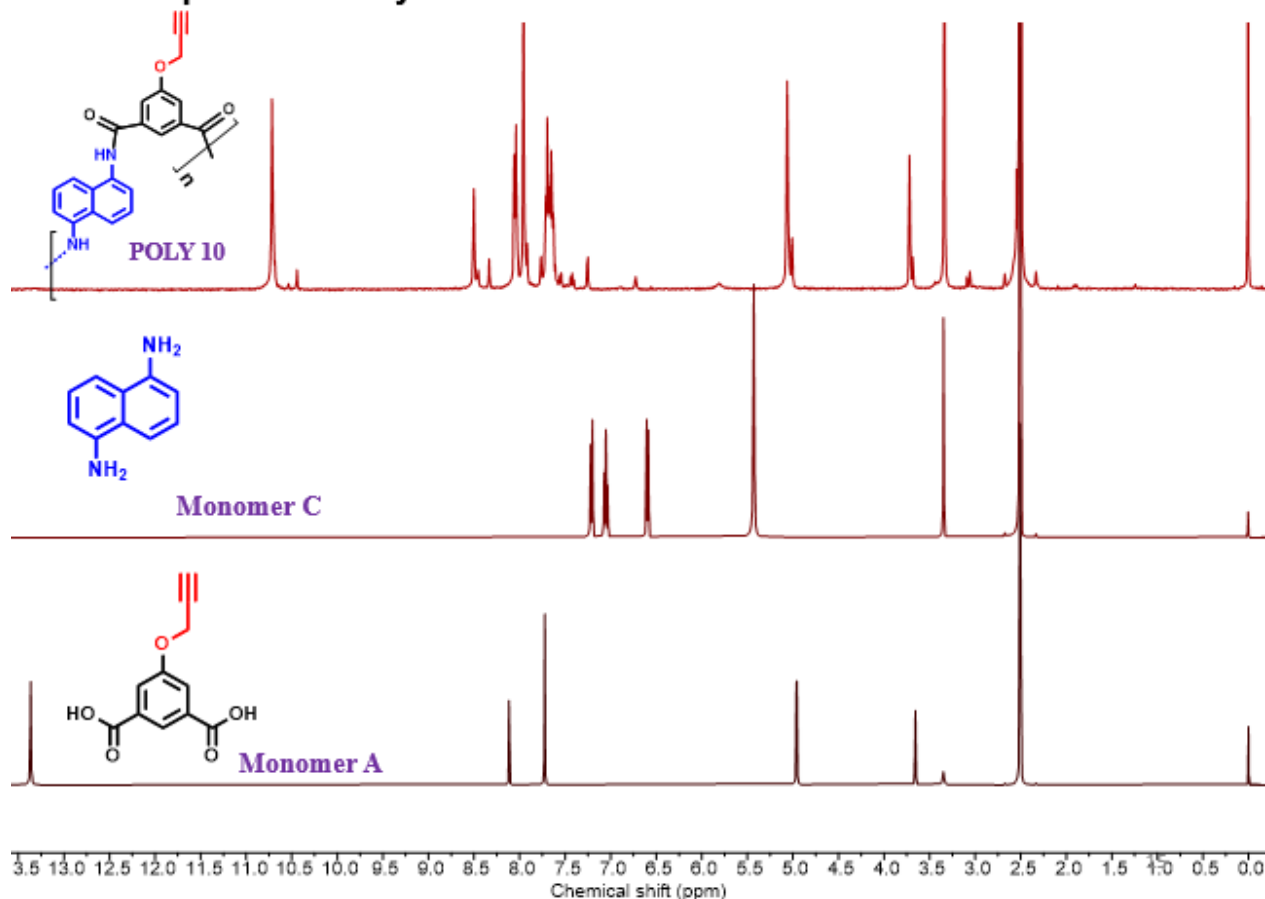
ppm, the aromatic region of 1,5-diaminonaphthalene, and **monomer A** shows a peak in the range of 7.5-8.6 ppm. The peaks at 4.99 ppm and 3.69 ppm correspond to the methylene ( $-\text{CH}_2$ ) group and terminal hydrogen ( $-\text{CH}$ ) of propargylic group protons.  $^1\text{H}$  NMR spectroscopic studies of the polymer provide evidence of the formation of intramolecular hydrogen bonding between monomer units in DMSO solvent. It is observed that amide proton ( $-\text{NH}$ ) undergoes a considerable downfield shift due to the formation of intramolecular hydrogen bonding in the case of **POLY 11**.

**$^1\text{H}$  NMR spectra of Poly 11 in DMSO:**



(a)

**$^1\text{H}$  NMR spectra of Poly 10 in DMSO:**



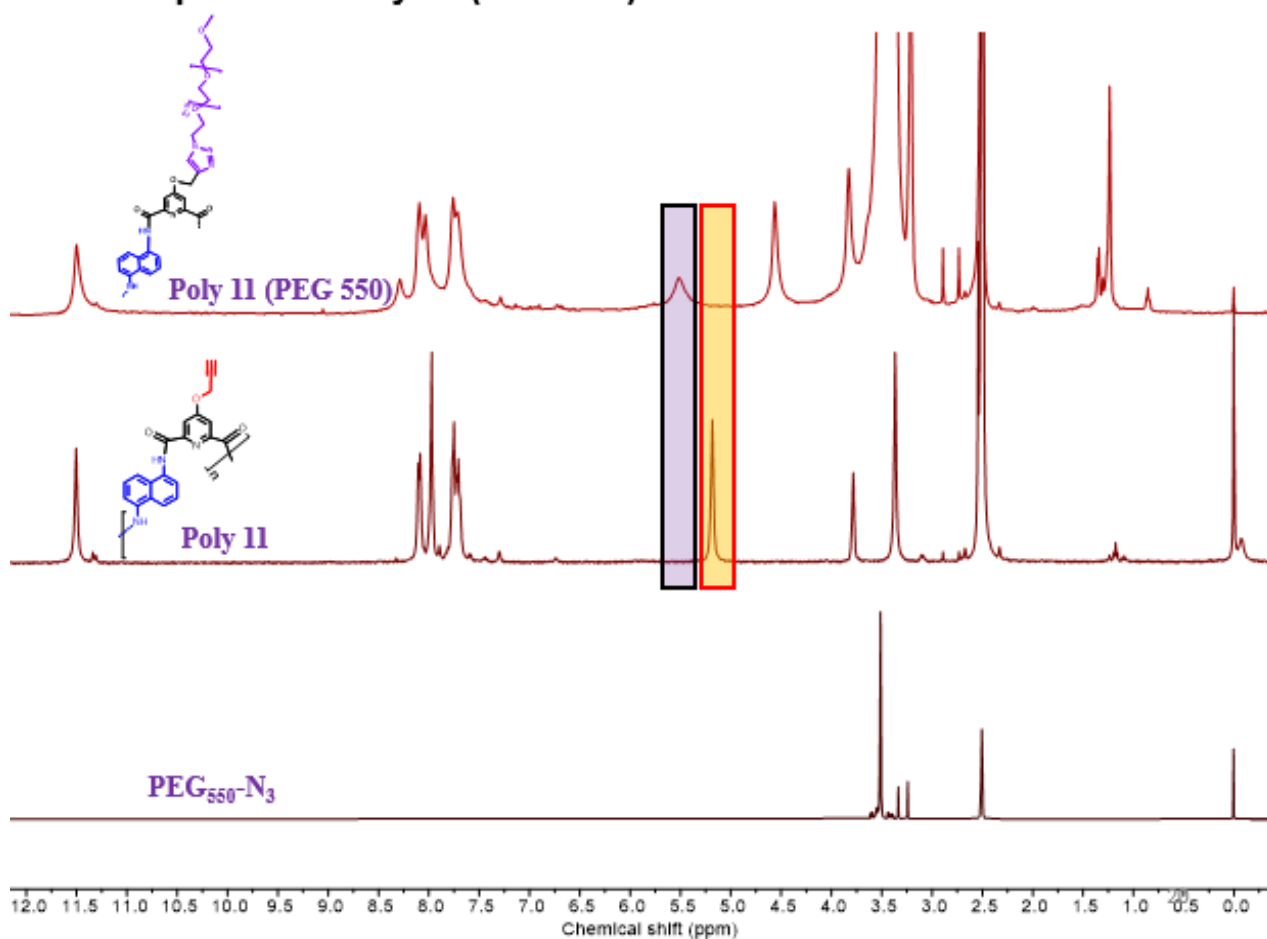
(b)

**Figure 11:**  $^1\text{H}$  NMR spectra of **POLY 11** and **POLY 10** in DMSO.

After developing a novel method for synthesizing these two polymers, the post-polymerization modification was done at the Propargyl group, acting as a reactive handle for further solubility improvement. However, to proceed with further studies, the polymers should be dissolved completely in a suitable organic solvent. From that point forward, we focused more on polymer solubility and ways to improve it. We perform a Copper-catalyzed azide-alkyne cycloaddition click reaction between the Propargyl groups and various monosubstituted long oxy ethyl chain azides to increase the solubility. The  $^1\text{H}$  NMR spectrum of the polymer after click reaction is shown in the figure below. Figure 12 (a) shows the spectra of **POLY 11 (PEG550)**

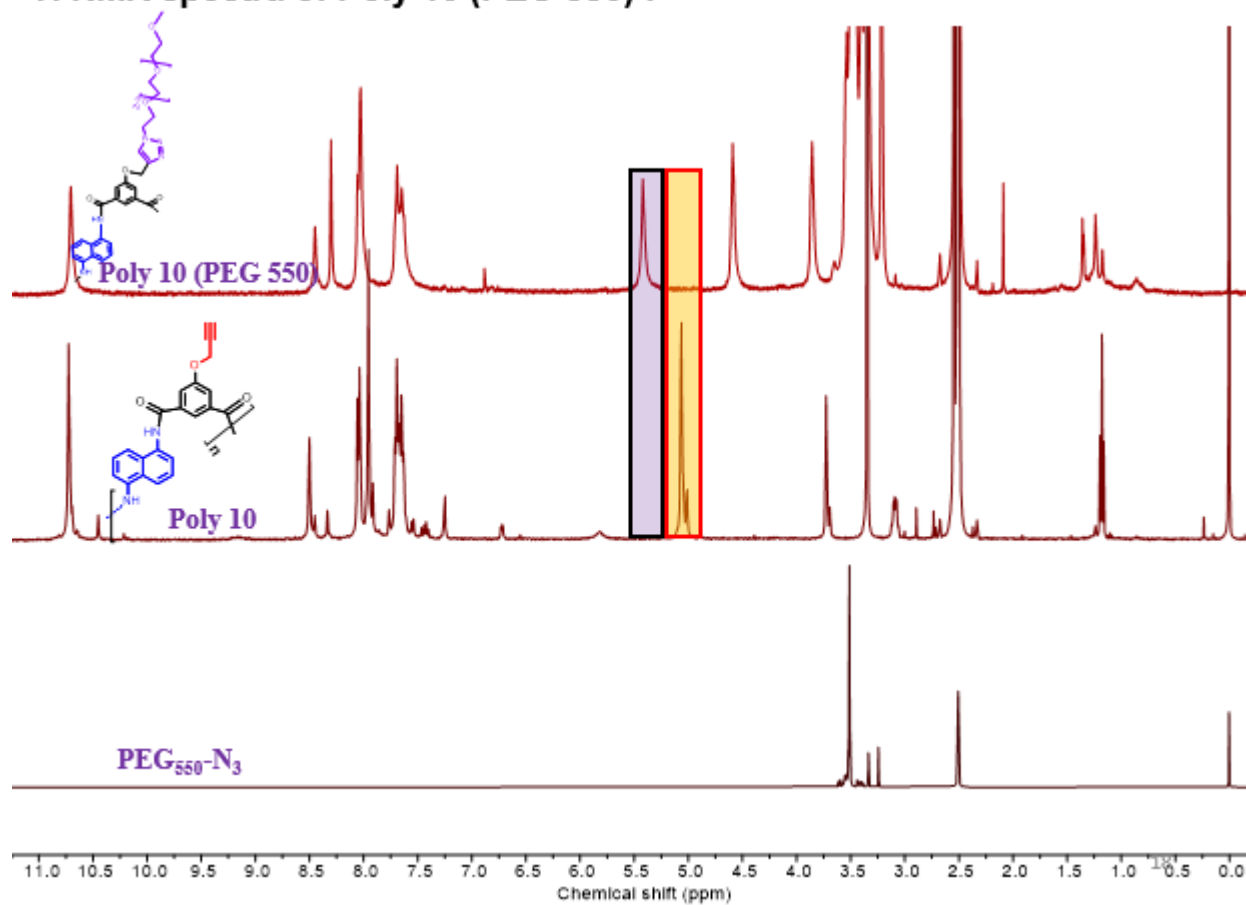
with the amide proton signal at 11.5-11.7 ppm. The aromatic region of 1, 5-diaminonaphthalene, and **monomer B** are in the range of 7.6-8.7 ppm. The disappearance of propargylic protons peak at 5.2 ppm indicates the complete occurrence of the CuAAC click reaction. The remaining peaks in the range of 3.3-3.8 ppm are from PEG550-N<sub>3</sub>. Figure 12 (b) shows the spectra of **POLY 10 (PEG550)** with the amide proton signal at 10.8-11.0 ppm. The aromatic region of 1, 5-diaminonaphthalene, and **monomer A** are in the range of 7.5-8.7 ppm. The complete disappearance of the methylene group's peak at 4.99 ppm indicates that the CuAAC click reaction has occurred. The rest of the peaks in the range of 3.2-3.7 ppm are from PEG550-N<sub>3</sub>.

### <sup>1</sup>H NMR spectra of Poly 11 (PEG 550) :



(a)

### <sup>1</sup>H NMR spectra of Poly 10 (PEG 550) :



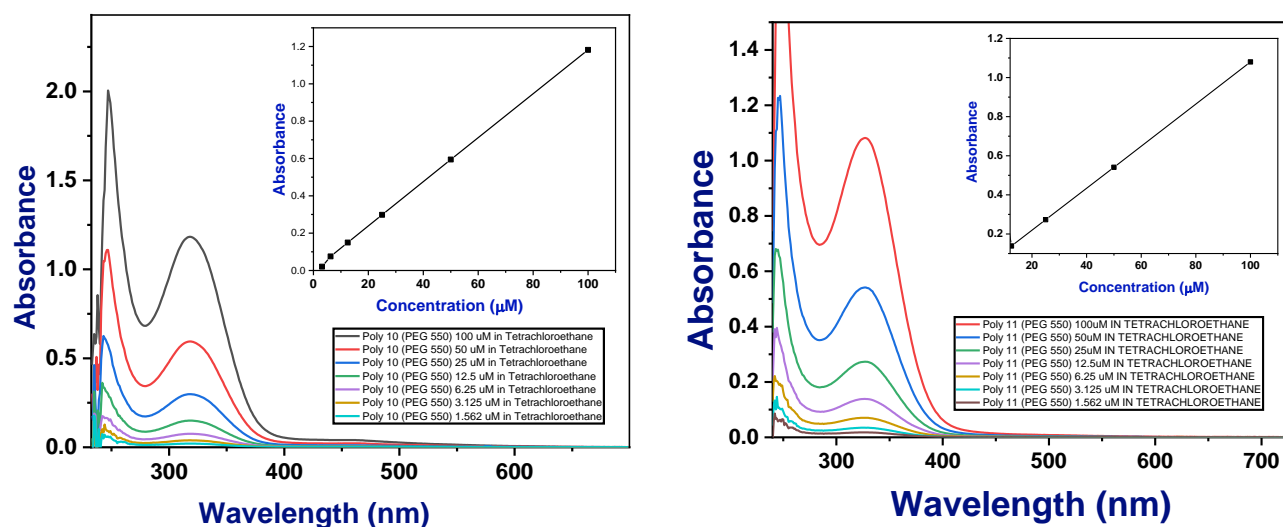
(b)

**Figure 12:** <sup>1</sup>H NMR of **POLY11** and **POLY 10** after CuAAc Click reaction in DMSO.

## 2.2 UV-Visible spectroscopic studies:

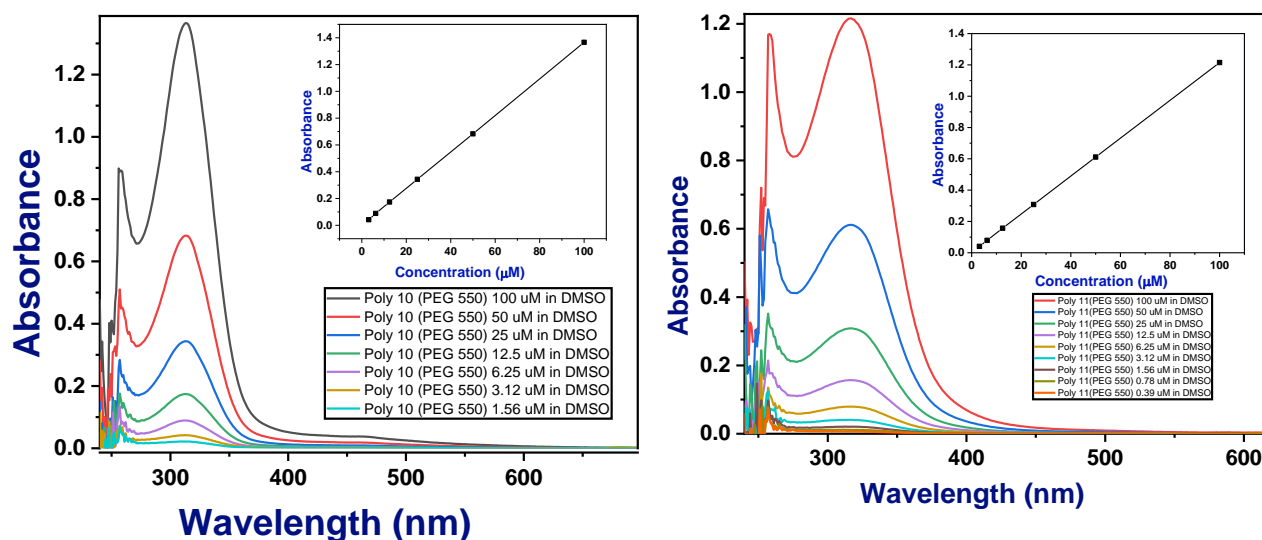
The UV-Vis absorption spectra of all compounds have been measured in DMSO and TCE solvent. How and where the molecule absorbs and emits light is influenced by molecule-solution and intermolecular interaction. When performing spectroscopic analysis, it's also crucial to be aware of the solution molarity. A molecule can have both intramolecular and intermolecular interactions. To reduce the possibility of intermolecular interactions between molecules, a low concentration solution is used for folding studies. For this reason, a low concentration solution is used, and spectroscopic analysis in a single-molecule state are carried as detailed below. All

the analysis of the POLY 10 and POLY 11 before and after post-polymerization modification are carried at 6.25  $\mu\text{M}$  concentration. The absorption spectra for the polymers at different concentrations in both solvents are displayed below. The linearity was determined by plotting concentration against the corresponding absorbance at wavelength 317 nm. The calibration curve showed linearity over a concentration range from 100  $\mu\text{M}$  to 1.56  $\mu\text{M}$  in both solvents TCE and DMSO. Here, the linearity clear indicates the whatever the concentration we are working is for the single-molecule phenomenon.



**Figure 13:** Absorption spectra of **POLY 10 (PEG 550)** and **POLY 11 (PEG550)** in TCE. Inset: The variation of absorbance vs. concentration follows Beer-Lamberts law.

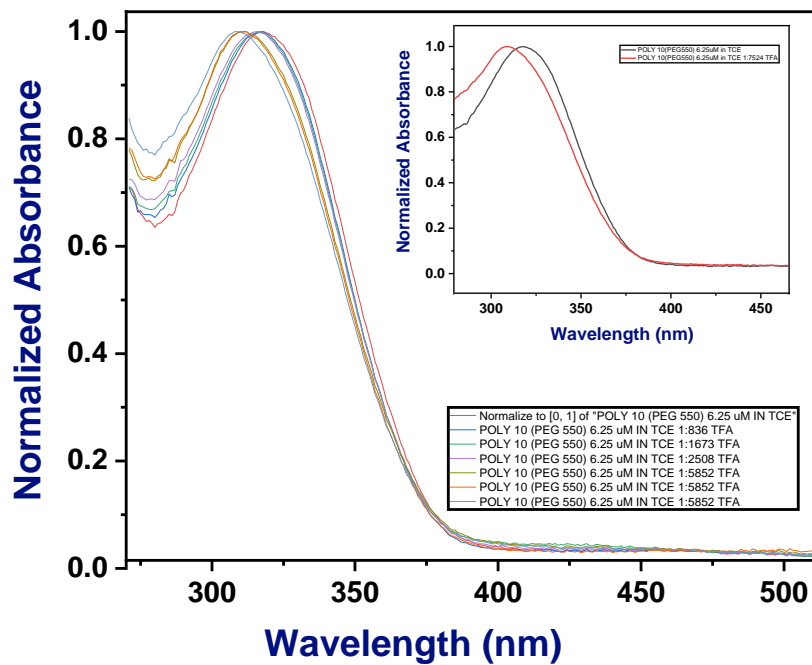
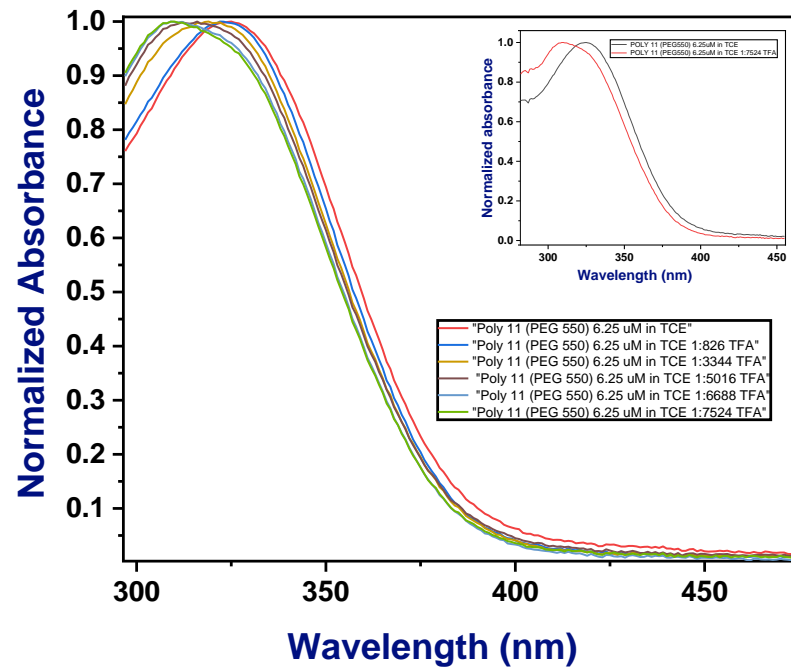




**Figure 14:** Absorption spectra of polymers **POLY 10(PEG 550)** and **POLY 11(PEG 550)** in DMSO. Inset: Calibration curve follows Beer-Lambert law.

### 2.2.1 Gradual addition of TFA

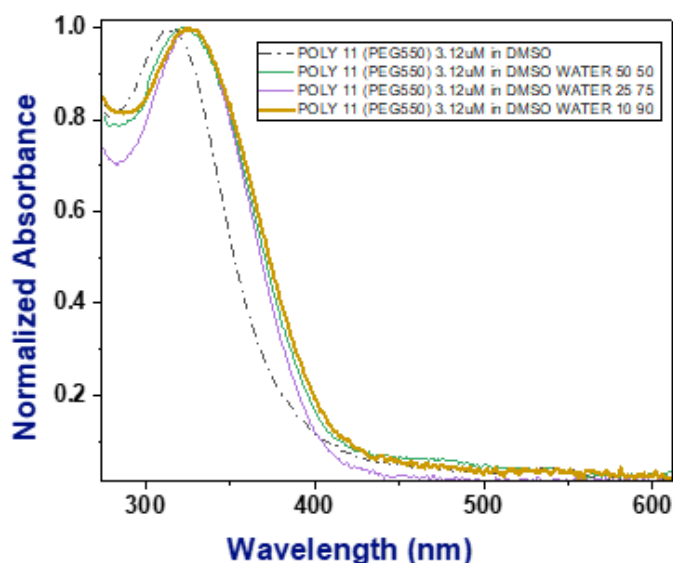
Trifluoroacetic acid (TFA) has the tendency to break the hydrogen bond and  $\pi$ - $\pi$  stacking in polymers. Modification in polymer by clicking with monosubstituted azide resulted in changes in polymer properties. The conformation of the polymer's chain in the solution state is pH-responsive. Increasing TFA concentration to the solution weakened the hydrogen bonds, causing the main chain to break or a folded structure into a relatively unfolded structure. **POLY 11** is a more folded structure than **POLY 10** because of intramolecular hydrogen bonding between amide proton & monomer moiety and  $\pi$ - $\pi$  stacking interactions. **POLY 10** is a folded structure because of only  $\pi$ - $\pi$  stacking. A significant shift of approx. 10 nm in **POLY 11** on the addition of TFA to it is due to the breakdown of a folded conformation of polymer, stabilized by non-covalent interactions (intramolecular hydrogen bonding,  $\pi$ - $\pi$  stacking) into a relatively unfolded structure as compared to **POLY 10**. The below figure depicts the more left-handed shift in **POLY 11** compared to **POLY 10** absorption spectra on the addition of TFA.



**Figure 15: POLY11 (PEG550) and POLY 10 (PEG 550) on the addition of TFA.**

### **2.2.2 Gradual addition of water to POLY 10(PEG 550) and POLY 11(PEG550) in DMSO**

The solvent effect plays an important role in the folding properties of a polymer. In these studies, polymers are dissolved in different DMSO and water ratios, and the shifts of their peak in UV-Vis absorption, wavelength maximum, are exploited to extract useful information. For instance, the formation of hydrogen bonds with solvent molecules. The UV-Vis peak absorption wavelengths of these polymers in different DMSO and water ratios are recorded at a concentration of 3.125  $\mu\text{M}$  to elucidate the nature of solvent and polymers interactions. This compound contains two parts; one is PEG 550, which is hydrophilic, and the other part is hydrophobic. The gradual addition of water to the hydrophilic part attracts the water molecule. The hydrophobic portion of the compound collapses into a more folded structure on the addition of water, i.e., the solvophobic effect. In **POLY11 (PEG550)**, the nitrogen introduced is expected to hydrogen bond to the neighboring amide hydrogens, i.e., more folded structure than **POLY 10 (PEG550)**. There is a combined effect (of intramolecular hydrogen bonding,  $\pi$ - $\pi$  stacking, and solvophobic effect) in **POLY 11 (PEG550)**. In **POLY 10 (PEG550)**, conformation is achieved only due to  $\pi$ - $\pi$  stacking and solvophobic effect. Equilibrium is attained at a higher concentration of water. The shift of peak on a higher water concentration to the right-hand side is due to the stable folded conformation achieved by a polymer.



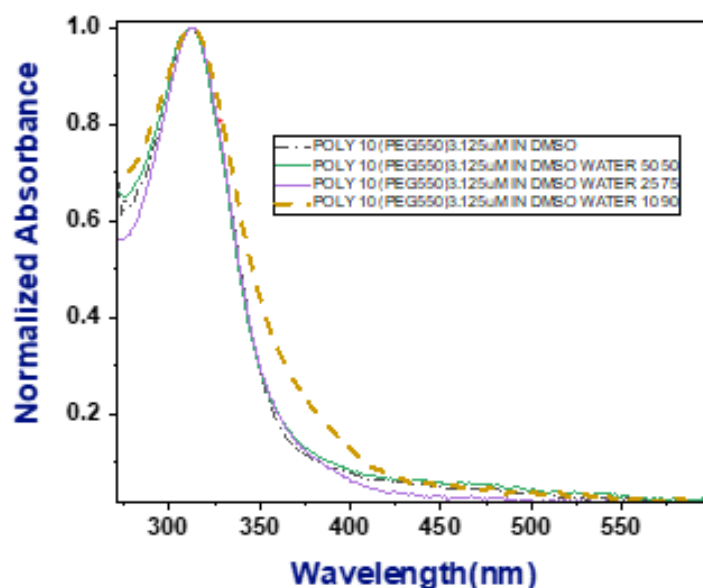
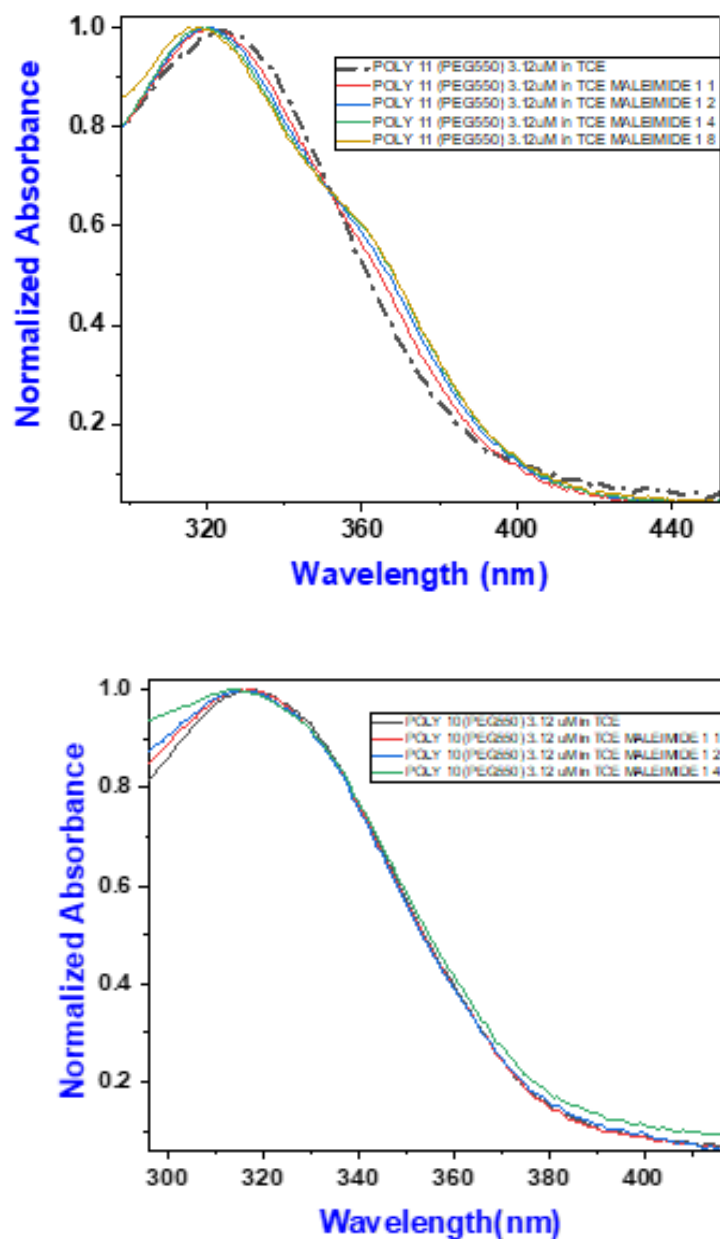


**Figure 16:** Absorption spectra of **POLY10 (PEG550)** and **POLY11 (PEG550)** in different DMSO and water ratios.

### **2.2.3 Addition of Maleimide to POLY10 (PEG550) and POLY 11 (PEG 550) in TCE.**

Maleimide is an unsaturated imide and an essential building block in organic synthesis. Here the polymer acts as a receptor that will accurately recognize a target guest molecule. The most crucial factor is that these two molecules should be structurally complementary to each other. **POLY 11 (PEG550)** has characteristic UV-Vis absorption spectra in the range of 300-500 nm (figure 17) with maxima around 323 nm. This peak corresponds to the absorbance band of the aromatic chromophore, and the band arises due to  $\pi$ - $\pi^*$  transitions of the molecule. Maleimide group contains NH donor, CO acceptor, NH donor (DAD) type, and **POLY 11** has CO acceptor, NH donor, CO acceptor (ADA) type, i.e., both are complementary to each other. Maleimide is expected to bind with **POLY11 (PEG550)** and fits into the hydrophobic cavity. Here, Maleimide is used as a template, and due to its complementary nature, it binds with **POLY 11**. The complexation of Maleimide to **POLY11 (PEG550)** causes a blue shift. And these spectral changes are not significantly shown in the case of **POLY10 (PEG550)** as the guest molecule Maleimide does not perfectly bind to it. These spectral changes result essentially from the interaction between the host and the guest molecule Maleimide, suggesting

the host-guest complex's formation. Mr.Subhendu Samanta has carried out this work.

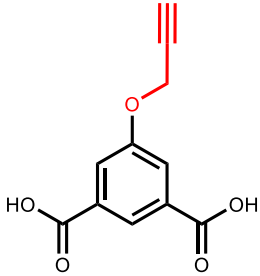
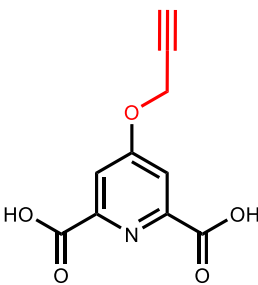
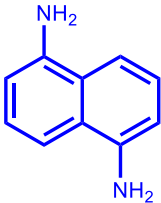


**Figure 17:** Absorption of Host-guest complexation of POLY 10 (PEG550) and POLY11 (PEG550) with Male

# Chapter 3

## Summary and Outlook

**Table 1:** Summary of the work.

	Monomer A	Monomer B
		
<b>Donor</b> 	<ul style="list-style-type: none"> <li>➤ POLY 10</li> <li>➤ Absence of intramolecular hydrogen bonding.</li> <li>➤ Predicted to be a random coil structure.</li> </ul> <p><b><u>After click reaction with PEG 550</u></b></p> <ul style="list-style-type: none"> <li>➤ Shows minor shift on the addition of TFA.</li> <li>➤ Host-guest complexation doesn't occur on the addition of Maleimide as a guest.</li> </ul>	<ul style="list-style-type: none"> <li>➤ POLY 11</li> <li>➤ Presence of intramolecular hydrogen bonding.</li> <li>➤ Predicted to be a stable folded structure.</li> </ul> <p><b><u>After click reaction with PEG 550</u></b></p> <ul style="list-style-type: none"> <li>➤ Shows more shift on the addition of TFA.</li> <li>➤ Host-guest complexation happens on the addition of Maleimide as a guest.</li> </ul>

The two different polymers, **POLY 10** and **POLY 11**, were successfully synthesized and characterized by  $^1\text{H}$  NMR, and photo physical properties were characterized by UV-Vis spectroscopy. **POLY 10** shows a prominent shift on the addition of TFA, which is lesser compared to **POLY 11**. The predicted folding properties of **POLY 11** are proved by the TFA experiment, the gradual addition of water in DMSO solution, Maleimide addition shows host-guest complexation because of intramolecular hydrogen bonding. The present results provide an efficient approach to generating helical superstructures through intramolecular conformational features induced by non-covalent interactions. In particular, the hydrogen bonding present in the structure leads to folding. Further, chirality can be induced in the foldamer design by adding a chiral fragment to it.

# Chapter 4

## Experimental section

### General information:

#### 4.1 Materials:

All the solvents and reagents used were purchased from commercial chemical suppliers Sigma Aldrich, Merck, TCI, avra and were used with further purification if needed. Solvents like DCM and methanol were distilled using standard distillation set up while HMPA and NMP were purified using kugelrohr apparatus. THF was dried over sodium and benzophenone as an indicator and distilled prior to use. Methanol and acetone were dried over  $K_2CO_3$ , DCM dried over phosphorous pentoxide, and distilled before use. HMPA, NMP were dried over calcium hydride and distilled using kugelrohr before use. DMF was dried over calcium sulfate and distilled under reduced pressure prior to use. Purification of products carried out by column chromatography using silica gel of mesh size 100-200  $\mu m$ . Thin-layer chromatography (TLC) was carried out on pre-coated plates. For visualization, UV light (254 nm) and ninhydrin stain used for nitrogen-containing compounds. Anhydrous sodium sulfate was used to dry the organic extracts, and solvents were removed by rotary evaporation under reduced pressure.

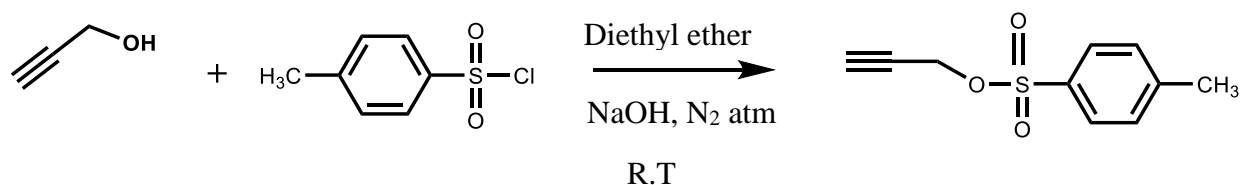
#### 4.2 Measurements:

The  $^1H$  NMR spectra were recorded on a 400 MHz Bruker Biospin Avance III FT-NMR spectrometer, respectively, with TMS as a standard at room temperature. The solvents used were  $CDCl_3$ , DMSO- $d_6$ . Chemical shift values ( $\delta$ ) are reported in parts per million (ppm), and Coupling constants (J) are reported in Hz. All spectra were calibrated using their residual solvent peak as internal reference:  $CDCl_3$  at 7.26 ppm,  $d_6$ -DMSO at 2.50 ppm. NMR data were processed using MestReNova software. UV-Vis was recorded on an Agilent Cary 5000 UV-Vis NIR spectrophotometer using quartz cuvettes of 1mm path length at 25°C. Molecular structures and reaction schemes were drawn using Chemdraw Professional 15.0.



## 4.3 Synthesis:

### 4.3.1 Synthesis of Propargyl p-toluene sulphonate:

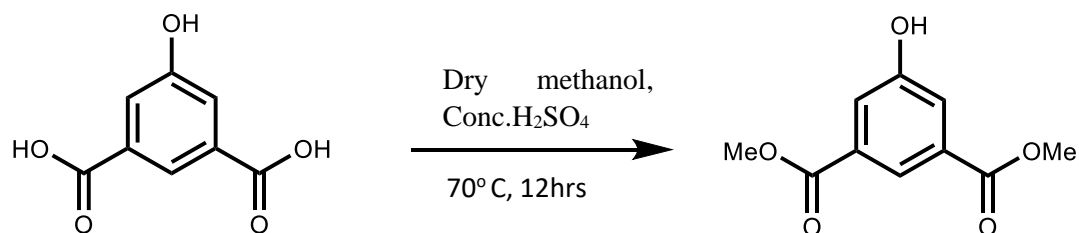


Propargyl alcohol ( 5 ml, 85.96 mmol), tosyl chloride (21.30 gm, 111.72 mmol) was dissolved in diethyl ether (90 ml) under N<sub>2</sub> atmosphere, and the solution was cooled to 0° C in an ice bath. Then NaOH pellets (17.89 gm, 448.3 mmol) were added in 6 portions. The reaction mixture was stirred at room temperature overnight. The suspension was poured into cold water (60 ml). Then aqueous layer was extracted with ether (2 times with 100 ml). The organic phase dried over anhydrous Na<sub>2</sub>SO<sub>4</sub>. The solvent was evaporated to give Propargyl tosylate as a dark color liquid.

Yield, 16 gm (88.8 %).

**<sup>1</sup>H NMR (400 MHz, CDCl<sub>3</sub>):** 7.8 (d, J = 14 Hz, 2 H), 7.4 (d, J = 14 Hz, 2 H), 4.8 (d, J = 21 Hz, 2 H), 2.5 (t, J = 23 Hz, 1 H), 2.4 (s, 3 H).

### 4.3.2 Synthesis of dimethyl 5-hydroxyisophthalate<sup>35</sup>:

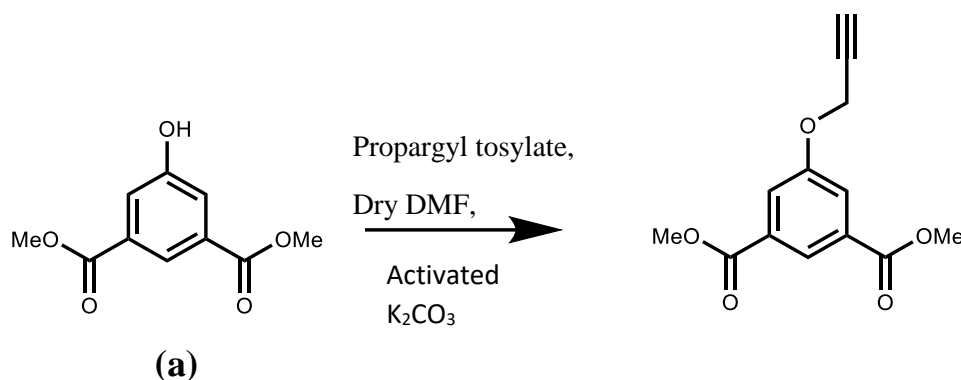


5-hydroxyisophthalic acid (10 gm, 54.91 mmol) dissolved in dry methanol (100 ml) with conc.  $\text{H}_2\text{SO}_4$  (1 ml). The reaction mixture was stirred at  $70^\circ\text{C}$  for 12 hours. Methanol was removed using a rotary evaporator. The obtained residue was dissolved in 100 ml 10%  $\text{NaHCO}_3$  solution + 30 ml  $\text{H}_2\text{O}$  and extracted with 200 ml ethyl acetate. Repeat the process three times. The separated organic layer was passed through anhydrous  $\text{Na}_2\text{SO}_4$  and dried thoroughly.

Yield, 10 gm (87 %).

**$^1\text{H}$  NMR (400 MHz,  $\text{CDCl}_3$ ):** 8.25 (t,  $J = 14$  Hz, 1 H), 7.79 (d,  $J = 14$  Hz, 2 H), 6.17 (s, 1 H), 3.95 (s, 6 H).

### 4.3.3 Synthesis of dimethyl 5-(prop2-yn-1-yloxy) isophthalate<sup>36</sup>:

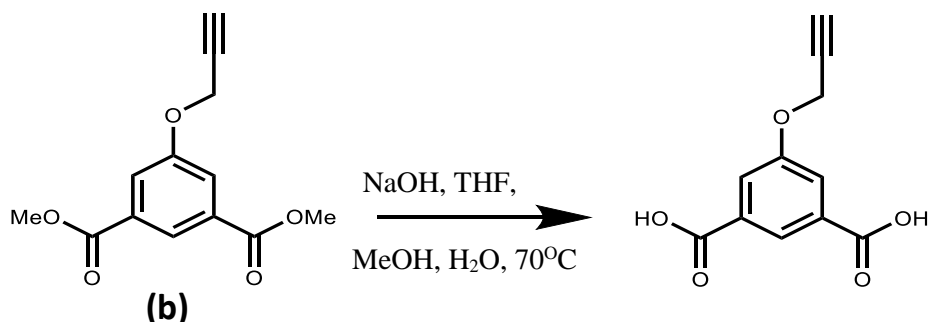


Compound a (4 gm, 19 mmol), Propargyl tosylate (5.84 gm, 27.78 mmol) was dissolved in dry DMF (100ml) and made the atmosphere inert through nitrogen purging. Then activated  $\text{K}_2\text{CO}_3$  (5.1 gm, 36.96 mmol) was added, heated the reaction mixture at  $70^\circ\text{C}$  for 4 hours, and then stirred at room temperature overnight. After that, the solution was filtered to remove excess  $\text{K}_2\text{CO}_3$ ; the filtrate was added dropwise to chilled water with vigorous stirring. Filtered the precipitate formed and dried thoroughly. The dried residue was dissolved in a minimum amount of chloroform and added dropwise to hexane in cold conditions. Then filtered and washed several times with hexane and dried.

Yield, 3.5 gm (74.5 %)

**$^1\text{H}$  NMR (400 MHz,  $\text{CDCl}_3$ ):** 8.35 (t,  $J = 14$  Hz, 1 H), 7.86 (t,  $J = 14$  Hz, 2 H), 4.81 (d,  $J = 24$  Hz, 2 H), 3.97 (s, 6 H), 2.57 (t,  $J = 24$  Hz, 1 H).

#### 4.3.4 Synthesis of 5-(prop-2-yn-1-yloxy) isophthalic acid<sup>36</sup>:

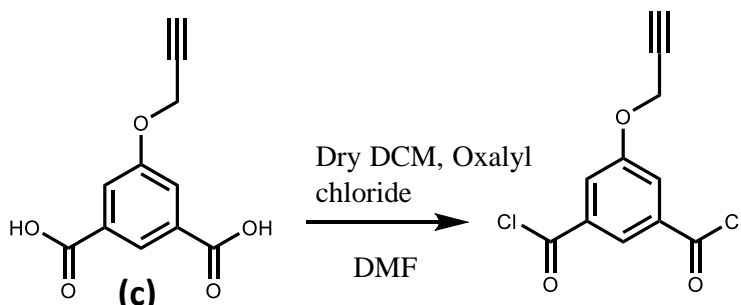


Into a 100 mL single-necked round bottom flask equipped with a magnetic stirring bar and a reflux condenser were charged with dimethyl-5-(propargyloxy)isophthalate (1 gm, 4.032 mmol), THF (8 ml), sodium hydroxide (0.806 gm, 20.16 mmol), water (8 mL), methanol (8 mL), and the reaction mixture was stirred at 70° C for 3hrs. The solution was cooled to room temperature and acidified with concentrated HCl. The product was isolated by filtration, washed with water, and dried at 80 °C under vacuum for 12 hrs.

Yield, 0.62 gm (69.87%)

**<sup>1</sup>H NMR (400 MHz, DMSO):** 13.37 (s, 2 H), 8.11 (t, J = 13 Hz, 1 H), 7.72 (d, J = 13 Hz, 2 H), 4.96 (d, J = 23 Hz, 2 H), 3.66 (t, J = 23 Hz, 1 H).

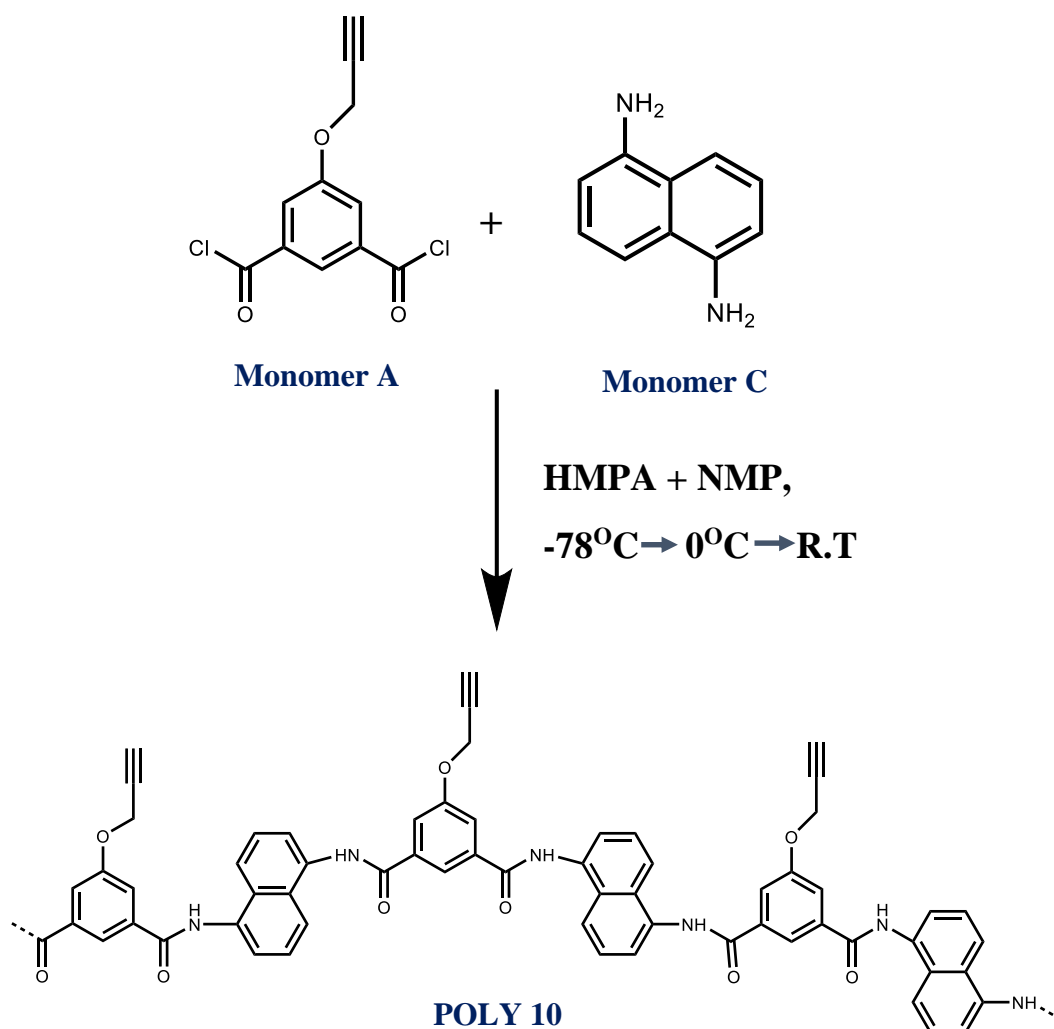
#### 4.3.5 Synthesis of 5-(prop-2-yn-1-yloxy) isophthaloyl dichloride:



Compound c (200 mg, 0.92 mmol) was dissolved in dry DCM (16 ml) after nitrogen purging. Oxalyl chloride (0.6 ml, 4.60 mmol), dry DMF (3 drops) were added to the reaction mixture. The reaction mixture was stirred for 4hrs. The solvent was removed under reduced pressure.

Quantitative yield.

#### 4.3.6 Synthesis of POLY 10:

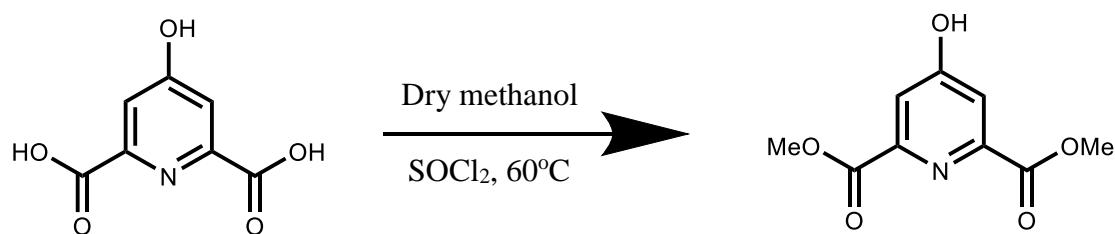


Monomer A (238.14 mg, 0.926 mmol) obtained as a quantitative yield was dissolved in 3 ml DCM. 1, 5-diaminonaphthalene (144.59 mg, 0.914 mmol) was dissolved in 1.4 ml NMP, 2.7 ml HMPA, and the solution was freeze to -78° C. In this frozen condition, the monomer A solution was transferred through a cannula to the previous one. After addition, the reaction mixture was stirred in ice-cold conditions for 4 hrs, followed by stirring at room temperature for 24 hrs. Later on, it was poured into 40 ml of water, and the yellowish precipitate formed immediately. The precipitate was filtered out using the Buchner apparatus and washed with water, acetone, and dried under vacuum. Then the dried polymer was dissolved in DMSO and precipitate out in chloroform. Then simple filtration was done, dried, and repeated three times.

Yield, 320 mg (35.9 %).

**<sup>1</sup>H NMR (400 MHz, DMSO):** 10.66 (s, J = 12.1 Hz, 2 H), 8.43 (t, J = 18.6 Hz, 1 H), 8.00 (d, J = 8.1 Hz, 2 H), 7.89 (d, J = 15.0 Hz, 2 H), 7.61 (ddd, J = 30.3, 19.3, 9.7 Hz, 4 H), 4.99 (d, J = 17.5 Hz, 2 H), 3.67 (t, J = 8.2 Hz, 1 H)

#### **4.3.7 Synthesis of Dimethyl 4-hydroxy pyridine-2, 6-dicarboxylate<sup>37</sup>:**

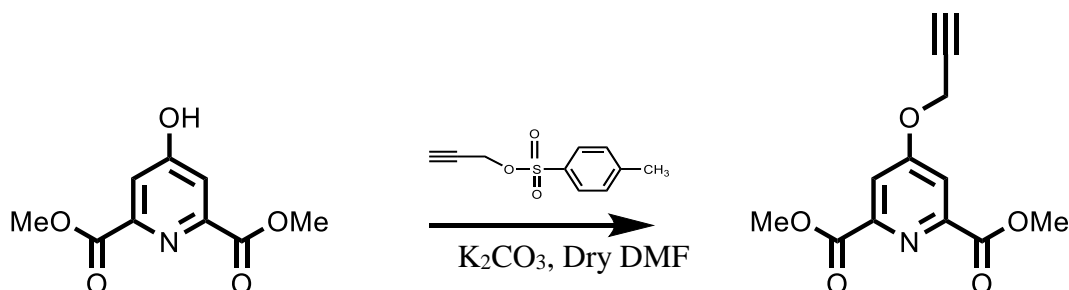


Chelidamic acid (2.5 gm, 13.65 mmol) dissolved in dry methanol (100 ml). N<sub>2</sub> purging was done for 10 minutes, and the solution was cooled down to 0° C in an ice bath. Thionyl chloride (SOCl<sub>2</sub>) (2.5 ml) was added to the solution in ice-cold conditions. The reaction mixture was stirred at 60° C overnight. The solvent was evaporated and quenched with chilled water. Extraction was done three times with chloroform (70 ml, 50 ml, and 50 ml). The combined organic layer was washed with brine solution and dried over anhydrous Na<sub>2</sub>SO<sub>4</sub>. The solvent was evaporated with a rotary evaporator to give a white color solid.

Yield, 2.27 gm (78.8 %).

**<sup>1</sup>H NMR (400 MHZ, DMSO-d<sub>6</sub>):** 11.62 (s, 1 H), 7.59 (s, 2 H), 3.93 (m, 6 H)

#### **4.3.8 Synthesis of Dimethyl 4-(prop-2-yn-1-yloxy) pyridine-2,6-dicarboxylate<sup>38</sup>:**

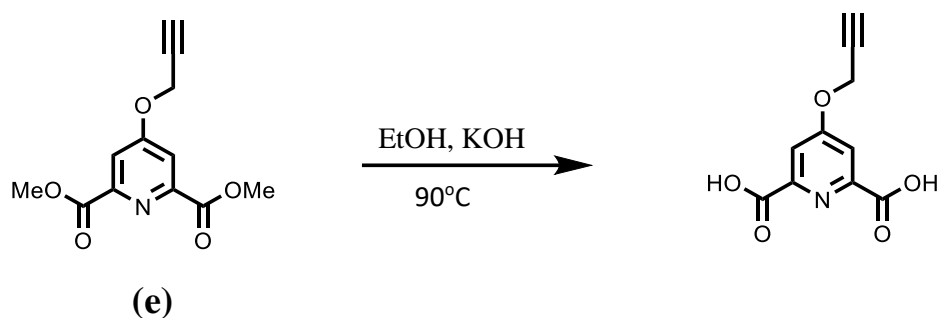


Compound d (2 gm, 9.47 mmol), Propargyl tosylate (2.39 ml, 13.82 mmol) were dissolved in dry DMF (50 ml). After that, activated  $K_2CO_3$  was added to the reaction mixture. The solution was stirred at 90° C for four hours then stirred at room temperature overnight. Dropwise add the reaction mixture to chilled water to precipitate out the compound. The obtained solution was filtered and dried. The compound was dissolved in chloroform (suitable solvent) for crystallization, and then excess hexane was added to precipitate the compound. Then obtained solution was filtered and the obtained precipitate dried in the oven.

Yield, 1.62 gm (68.8%).

**<sup>1</sup>H NMR (400MHz, DMSO-d<sub>6</sub>):** 7.8 (s, 2 H), 5.2 (d, J = 14 Hz, 2 H), 3.8 (s, 6 H), 3.68 (s, 1 H).

#### 4.3.9 Synthesis of 4-(prop-2yn-1-yloxy) pyridine-2, 6-dicarboxylic acid<sup>39</sup>:

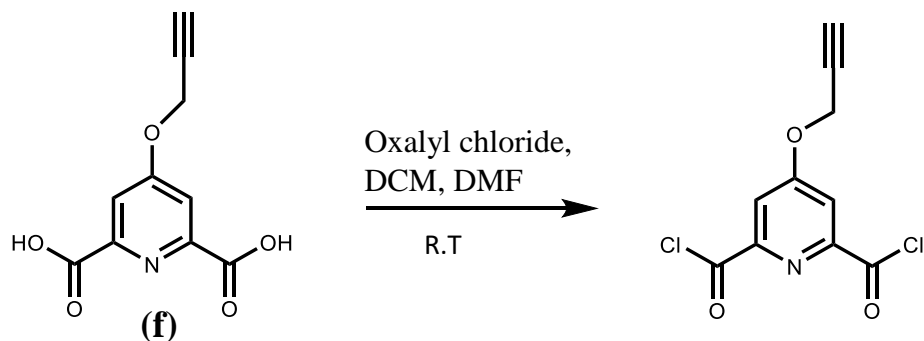


Compound e (1.7 gm, 6.82 mol), KOH (1.53 gm, 27.308 mol) were dissolved in ethanol (50 ml). The reaction mixture was stirred at 90° C for 1 hour. Ethanol was removed completely using a rotary evaporator. Then the residue was dissolved in a minimal amount of water and acidified by 1N HCl solution. The solution was filtered, and the obtained residue was dried thoroughly.

Yield, 1.12 gm (72.9%).

**<sup>1</sup>H NMR (400MHz, DMSO-d<sub>6</sub>):** 13.40 (s, 1 H), 7.79 (s, 2 H), 5.11 (d, 2 H, J = 21 Hz), 3.76 (s, 1 H).

#### 4.3.10 Synthesis of 4-(prop-2yn-1-yloxy) pyridine-2, 6-dicarbonyl dichloride:

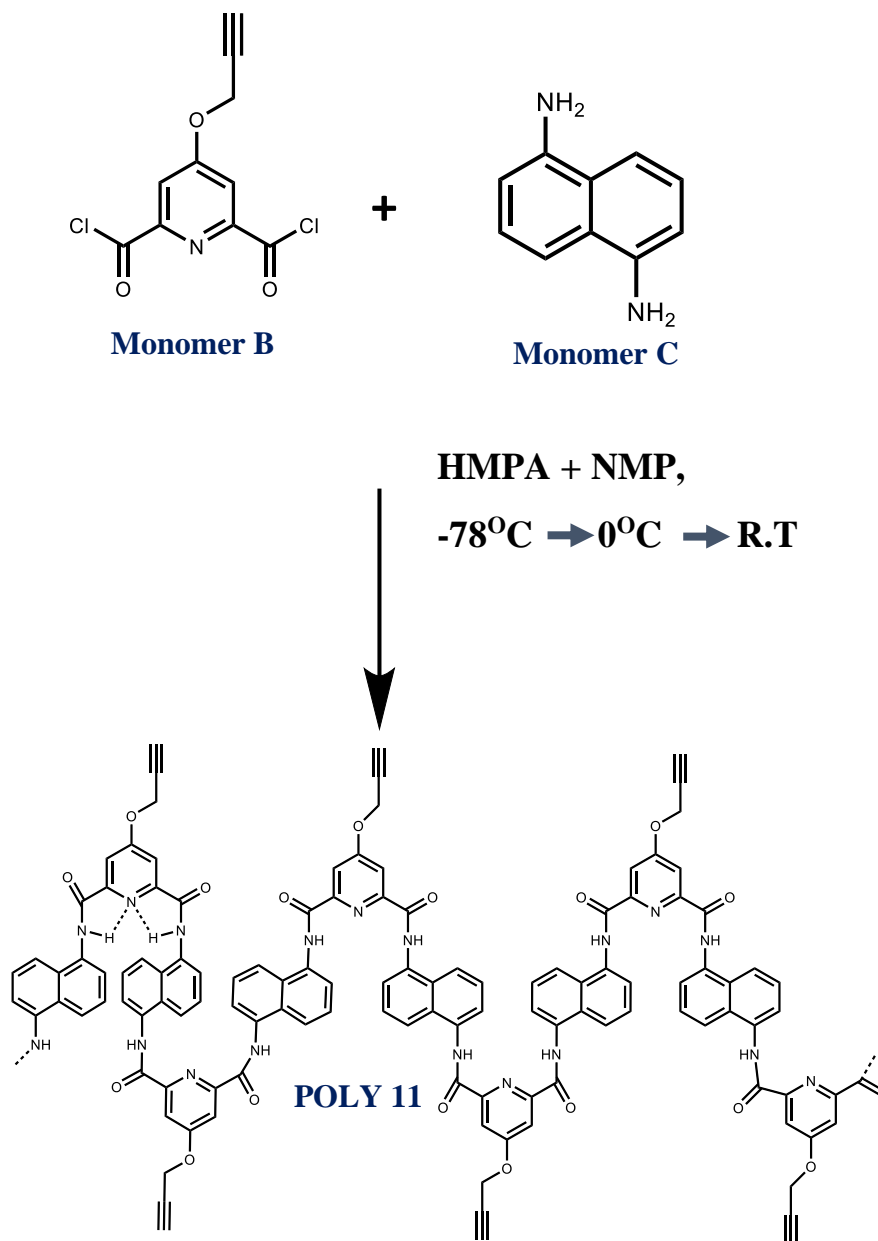


Compound f (200 mg, 0.92 mmol) was dissolved in dry DCM (16 ml) after nitrogen purging. Oxalyl chloride (0.6 ml, 4.601 mmol), dry DMF (3 drops) were added to

the reaction mixture. The reaction mixture was stirred at room temperature for 4hrs. The solvent was removed under reduced pressure.

Quantitative yield.

#### 4.3.11 Synthesis of POLY 11:



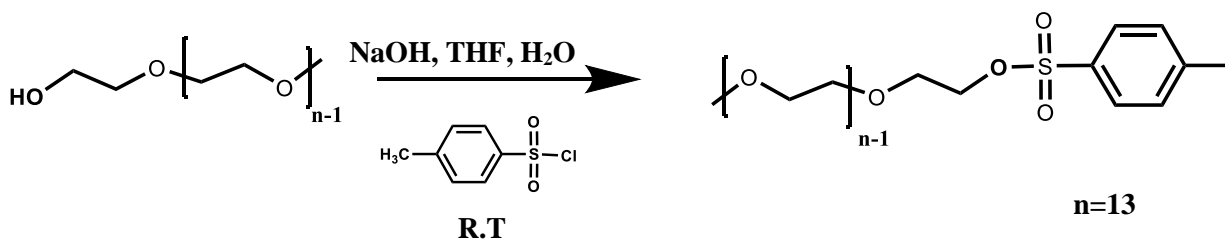


Monomer B (238.14 mg, 0.926 mmol) obtained as a quantitative yield was dissolved in 3 ml DCM. 1, 5-diaminonaphthalene (144.59 mg, 0.914 mmol) was dissolved in 1.4 ml NMP, 2.7 ml HMPA, and the solution was freeze to -78° C. In this frozen condition, the monomer A solution was transferred through a cannula to the previous one. After addition, the reaction mixture was stirred in ice-cold conditions for 4hrs, followed by stirring at room temperature for 24 hrs. Later on, it was poured into 40 ml of water, and the yellowish precipitate formed immediately. The precipitate was filtered out using the Buchner apparatus and washed with water, acetone, and dried under vacuum. Then the dried polymer was dissolved in DMSO and precipitate out in chloroform. Then simple filtration was done, dried, and repeated three times.

Yield, 300 mg (34 %).

**<sup>1</sup>H NMR (400 MHz, DMSO):** 11.5 (s, J = 12.1 Hz, 2 H), 8.43 (d, J = 8.1 Hz, 2 H), 7.89 (d, J = 15.0 Hz, 2 H), 7.61 (ddd, J = 30.3, 19.3, 9.7 Hz, 4 H), 5.2 (d, J = 17.5 Hz, 2 H), 3.67 (t, J = 8.2 Hz, 1 H)

#### 4.3.12 Synthesis of PEG550-tosylate:

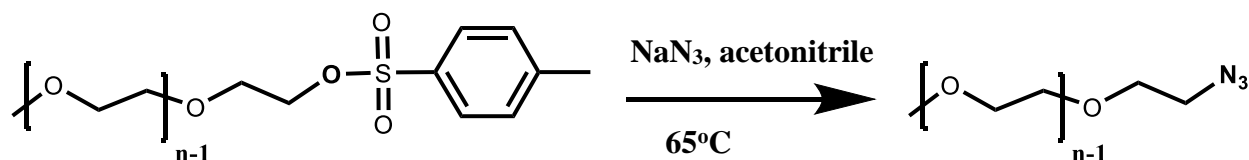


PEG550 (10 gm, 18.18 mmol) was dissolved in 15 ml THF. Then the solution of NaOH was added dropwise to the mixture in ice-cold conditions. P-toluenesulphonyl chloride (5.2 gm, 27.27 mmol) was dissolved in 10 ml THF and added to the reaction mixture for 1 hr dropwise. The reaction mixture was stirred at room temperature overnight. The organic layer was separated, and then the aqueous layer was washed with diethyl ether three times. Then combined organic layer was washed with 10% NaOH solution and dried over anhydrous Na<sub>2</sub>SO<sub>4</sub>. The yellowish color liquid product was obtained.

Yield, 5.1 gm (39.8 %).

**<sup>1</sup>H NMR (400MHz, CDCl<sub>3</sub>):** 7.79 (d, J = 8.3 Hz, 1 H), 7.34 (d, J = 8.1 Hz, 1 H), 4.16 (dd, J = 10.1, 5.4 Hz, 1 H), 3.83 – 3.47 (m, 24 H), 3.42 (d, J = 36.3 Hz, 2 H), 2.45 (s, 3 H).

#### 4.3.13 Synthesis of PEG550-N<sub>3</sub>:

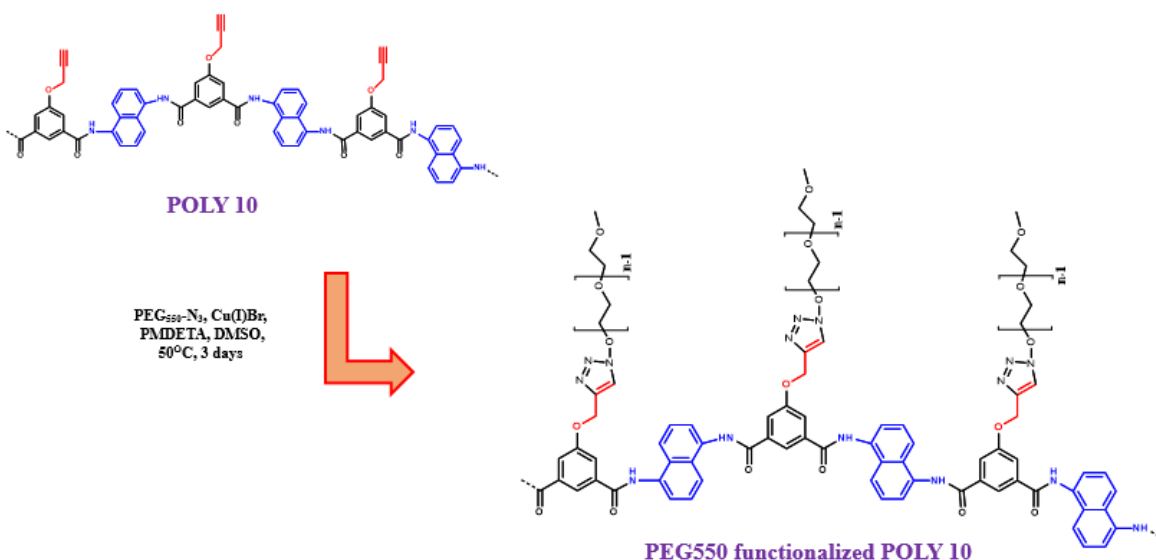


PEG550-OTs (5.1 gm, 7.24 mmol) was dissolved in 130 ml acetonitrile and N<sub>2</sub> purged through condenser 3-4 times. Then NaN<sub>3</sub> (1.82 gm, 28.96 mmol) was added and stirred at 65°C for two days. The solvent was removed using a rotary evaporator. The organic layer separated using diethyl ether and dried over anhydrous Na<sub>2</sub>SO<sub>4</sub>. The whitish liquid product was obtained.

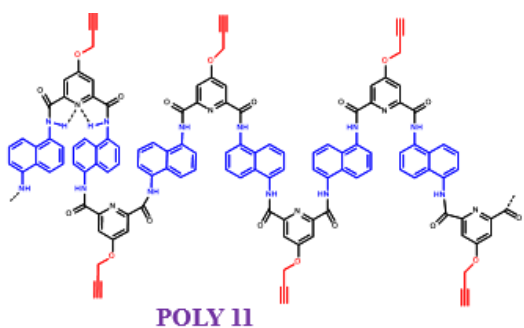
Yield, 1.5 gm (36.4 %)

**<sup>1</sup>H NMR (400MHz, CDCl<sub>3</sub>):** 3.77 – 3.60 (m, 1H), 3.61 – 3.49 (m, 1H), 3.42 – 3.26 (m, 1H).

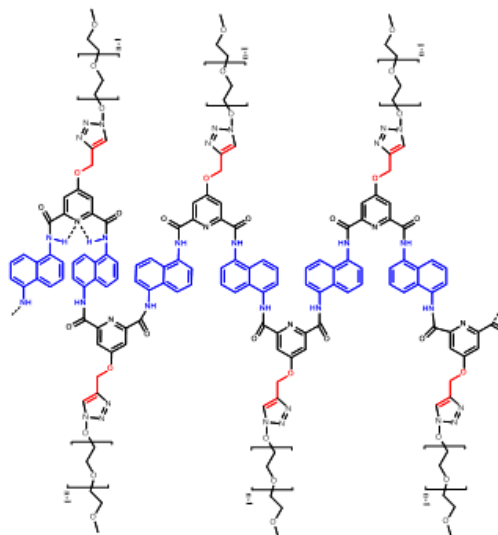
#### 4.3.14 Synthesis of click reaction of POLY10 and PEG550-N<sub>3</sub>.



#### 4.3.15 Synthesis of click reaction of POLY 11 and PEG550-N3.



PEG<sub>550</sub>-N<sub>3</sub>, Cu(I)Br,  
PMDETA, DMSO,  
50°C, 3 days



PEG550 functionalized POLY 11

# References

1. Ghosh, S., & Ramakrishnan, S. (2005). Small-Molecule-Induced Folding of a Synthetic Polymer. *Angewandte Chemie*, 117(34), 5577-5583.
2. Wulff, G. (2002). Enzyme-like catalysis by molecularly imprinted polymers. *Chemical reviews*, 102(1), 1-28.
3. Ghosh, S., & Ramakrishnan, S. (2004). Aromatic Donor-Acceptor Charge-Transfer and Metal-Ion-Complexation-Assisted Folding of a Synthetic Polymer. *Angewandte Chemie*, 116(25), 3326-3330.
4. Hill, D. J., Mio, M. J., Prince, R. B., Hughes, T. S., & Moore, J. S. (2001). A field guide to foldamers. *Chemical Reviews*, 101(12), 3893-4012.
5. Gellman, S. H. (1998). Foldamers: a manifesto. *Accounts of Chemical Research*, 31(4), 173-180.
6. Deshayes, K., Broene, R. D., Chao, I., Knobler, C. B., & Diederich, F. (1991). Synthesis of the helicopodands: novel shapes for chiral clefts. *The Journal of Organic Chemistry*, 56(24), 6787-6795.
7. Paruch, K., Katz, T. J., Incarvito, C., Lam, K. C., Rhatigan, B., & Rheingold, A. L. (2000). First friedel– Crafts diacylation of a phenanthrene as the basis for an efficient synthesis of nonracemic [7] helicenes. *The Journal of organic chemistry*, 65(22), 7602-7608.
8. Fuji, K., Furuta, T., & Tanaka, K. (2001). Synthesis of configurationally defined sexi-and octinaphthalene derivatives. *Organic letters*, 3(2), 169-171.
9. Green, MM, Park, JW, Sato, T., Teramoto, A., Lifson, S., Selinger, RL, & Selinger, JV (1999). The macromolecular route to chirality amplification. *Angewandte Chemie* , 111 (21), 3328-3345.
10. Lin, L. N., & Brandts, J. F. (1980). Kinetic mechanism for conformational transitions between poly-L-prolines I and II: a study utilizing the cis-trans specificity of a proline-specific protease. *Biochemistry*, 19(13), 3055-3059.
11. Noe, C. R., Miculka, C., & Bats, J. W. (1994). On the helicity of oligomeric formaldehyde. *Angewandte Chemie International Edition in English*, 33(14), 1476-1478.
12. Zimm, B. H., & Bragg, J. K. (1959). Theory of the phase transition between helix and random coil in polypeptide chains. *The journal of chemical physics*, 31(2), 526-535
13. Poland, D., & Scheraga, H. A. (1970). Theory of helix-coil transitions in biopolymers.

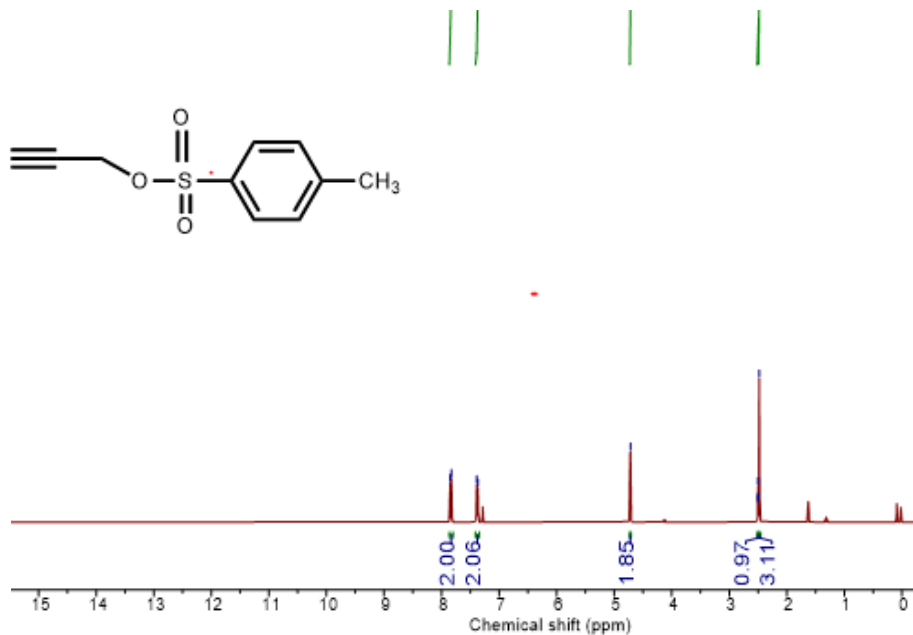
14. Jackson, S. E. (1998). How do small single-domain proteins fold?. *Folding and Design*, 3(4), R81-R91
15. Arunan, E., Desiraju, G. R., Klein, R. A., Sadlej, J., Scheiner, S., Alkorta, I., ... & Nesbitt, D. J. (2011). Definition of the hydrogen bond (IUPAC Recommendations 2011). *Pure and applied chemistry*, 83(8), 1637-1641.
16. Meudtner, R. M., Ostermeier, M., Goddard, R., Limberg, C., & Hecht, S. (2007). Multifunctional “clickates” as versatile extended heteroaromatic building blocks: efficient synthesis via click chemistry, conformational preferences, and metal coordination. *Chemistry—A European Journal*, 13(35), 9834-9840
17. Xu, Y. X., Wang, G. T., Zhao, X., Jiang, X. K., & Li, Z. T. (2009). Folding of aromatic amide-based oligomers induced by benzene-1, 3, 5-tricarboxylate anion in DMSO. *The Journal of organic chemistry*, 74(19), 7267-7273.
18. Lokey, R. S., & Iverson, B. L. (1995). Synthetic molecules that fold into a pleated secondary structure in solution. *Nature*, 375(6529), 303-305.
19. Saraogi, I., & Hamilton, A. D. (2009). Recent advances in the development of aryl-based foldamers. *Chemical Society Reviews*, 38(6), 1726-1743.
20. Fischer, L., Claudon, P., Pendem, N., Miclet, E., Didierjean, C., Ennifar, E., & Guichard, G. (2010). The Canonical Helix of Urea Oligomers at Atomic Resolution: Insights Into Folding-Induced Axial Organization. *Angewandte Chemie International Edition*, 49(6), 1067-1070.
21. Zhang, D. W., Wang, W. K., & Li, Z. T. (2015). Hydrogen-Bonding-Driven Aromatic Foldamers: Their Structural and Functional Evolution. *The Chemical Record*, 15(1), 233-251.
22. Zhu, J., Wang, X. Z., Chen, Y. Q., Jiang, X. K., Chen, X. Z., & Li, Z. T. (2004). Hydrogen-bonding-induced planar, rigid, and Zigzag oligoanthranilamides. synthesis, characterization, and self-assembly of a metallocyclophane. *The Journal of organic chemistry*, 69(19), 6221-6227.
23. C. A. Hunter and J. K. M. Sanders, *J. Am. Chem. Soc.*, 1990, **112**, 5525–5534.
24. Prest, P. J., Prince, R. B., & Moore, J. S. (1999). Supramolecular Organization of Oligo (m-phenylene ethynylene) s in the Solid-State. *Journal of the American Chemical Society*, 121(25), 5933-5939.
25. Luo, J., Wang, Y., & Nakano, T. (2018). Free-Radical Copolymerization of Dibenzofulvene with (Meth) acrylates Leading to  $\pi$ -Stacked Copolymers. *Polymers*, 10(6), 654.
26. Ikkanda, B. A., & Iverson, B. L. (2016). Exploiting the interactions of aromatic units for folding and assembly in aqueous environments. *Chemical Communications*, 52(50), 7752-7759.

27. Dill, K. A., Ozkan, S. B., Shell, M. S., & Weikl, T. R. (2008). The protein folding problem. *Annu. Rev. Biophys.*, 37, 289-316.
28. Merlet, E., Moreno, K., Tron, A., McClenaghan, N., Kauffmann, B., Ferrand, Y., & Olivier, C. (2019). Aromatic oligoamide foldamers as versatile scaffolds for induced circularly polarized luminescence at adjustable wavelengths. *Chemical Communications*, 55(66), 9825-9828.
29. Jiang, H., Léger, J. M., & Huc, I. (2003). Aromatic  $\delta$ -peptides. *Journal of the American Chemical Society*, 125(12), 3448-3449.
30. Tornøe, C. W., Christensen, C., & Meldal, M. (2002). Peptidotriazoles on solid phase: [1, 2, 3]-triazoles by regiospecific Copper (I)-catalyzed 1, 3-dipolar cycloadditions of terminal alkynes to azides. *The Journal of organic chemistry*, 67(9), 3057-3064.
31. Hein, J. E., & Fokin, V. V. (2010). Copper-catalyzed azide-alkyne cycloaddition (CuAAC) and beyond: new reactivity of copper (I) acetylides. *Chemical Society Reviews*, 39(4), 1302-1315.
32. Berl, V., Huc, I., Khoury, R. G., & Lehn, J. M. (2001). Helical Molecular Programming: Folding of Oligopyridine-dicarboxamides into Molecular Single Helices. *Chemistry—A European Journal*, 7(13), 2798-2809.
33. Berl, V., Krische, M. J., Huc, I., Lehn, J. M., & Schmutz, M. (2000). Template-induced and molecular recognition directed hierarchical generation of supramolecular assemblies from molecular strands. *CHEMISTRY-WEINHEIM-EUROPEAN JOURNAL*-, 6(11), 1938-1946.
34. Berl, V., Huc, I., Khoury, R. G., Krische, M. J., & Lehn, J. M. (2000). Interconversion of single and double helices formed from synthetic molecular strands. *Nature*, 407(6805), 720-723.
35. Verma, S., Maher, D. M., Nagane, S. S., Tawade, B. V., & Wadgaonkar, P. P. (2019). Thermally Crosslinkable and Chemically Modifiable Aromatic Polyesters Possessing Pendant Propargyloxy Groups. *Journal of Polymer Science Part A: Polymer Chemistry*, 57(5), 588-597.
36. Fredy, J. W., Scelle, J., Ramniceanu, G., Doan, B. T., Bonnet, C. S., Tóth, É., ... & Hasenknopf, B. (2017). Mechanostereoselective one-pot synthesis of functionalized head-to-head cyclodextrin [3] rotaxanes and their application as magnetic resonance imaging contrast agents. *Organic letters*, 19(5), 1136-1139.
37. Enel, M., Leygue, N., Saffon, N., Galaup, C., & Picard, C. (2018). Facile Access to the 12-Membered Macrocyclic Ligand PCTA and Its Derivatives with Carboxylate, Amide, and Phosphinate Ligating Functionalities. *European Journal of Organic Chemistry*, 2018(15), 1765-1773.

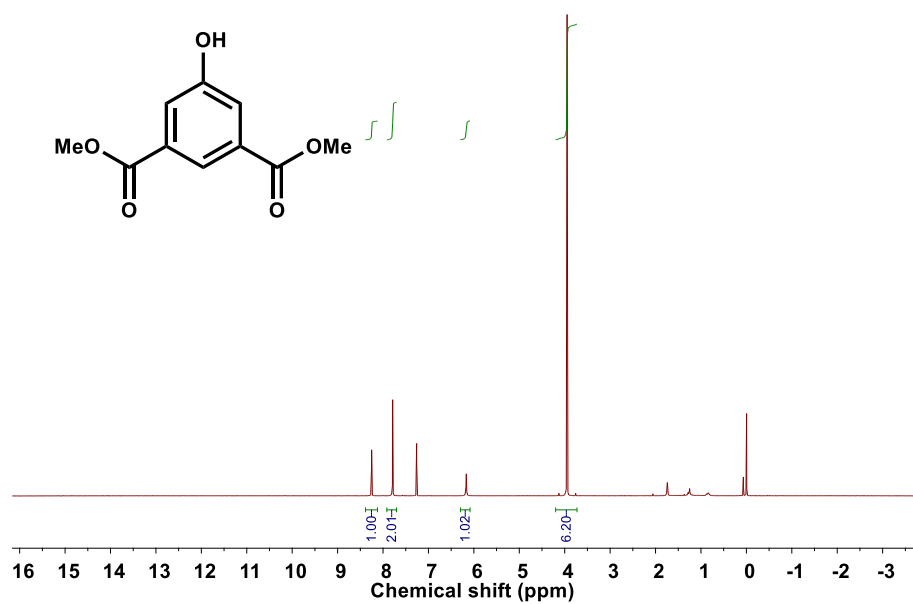
38. Tarasenko, E. A., & Beletskaya, I. P. (2016). Poly (ethylene glycol)-supported chiral pyridine-2, 6-bis (oxazoline): synthesis and application as a recyclable ligand in Cu-catalyzed enantioselective direct addition of terminal alkynes to imines. *Mendeleev Communications*, 6(26), 477-479.
39. Wang, F., Zhang, J., Ding, X., Dong, S., Liu, M., Zheng, B., ... & Huang, F. (2010). Metal coordination mediated reversible conversion between linear and cross-linked supramolecular polymers. *Angewandte Chemie International Edition*, 49(6), 1090-1094.

# Appendix

Propargyl p-toluene sulphonate,  $^1\text{H}$  NMR (400 MHz,  $\text{CDCl}_3$ ):

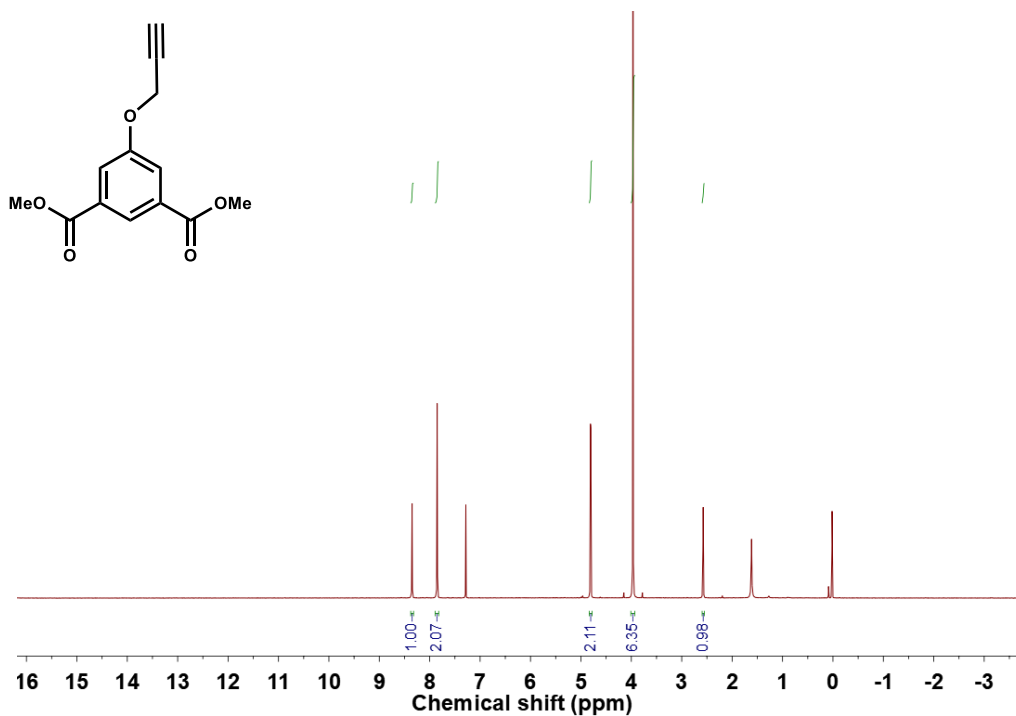


Dimethyl 5-hydroxyisophthalate,  $^1\text{H}$  NMR (400 MHz,  $\text{CDCl}_3$ ):

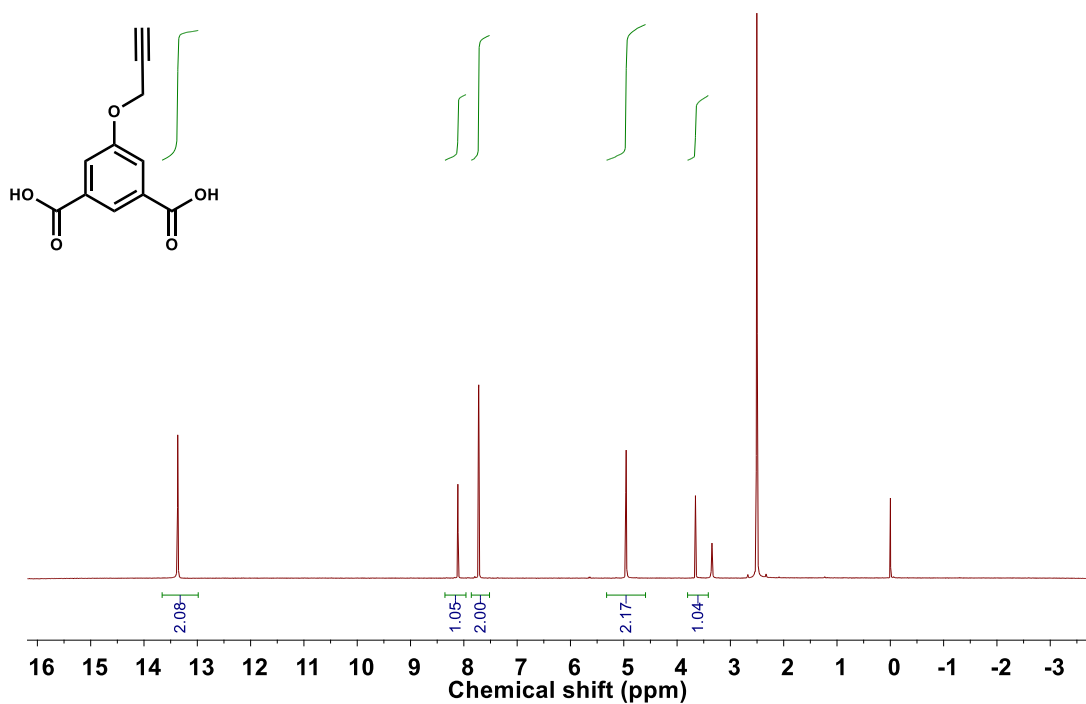




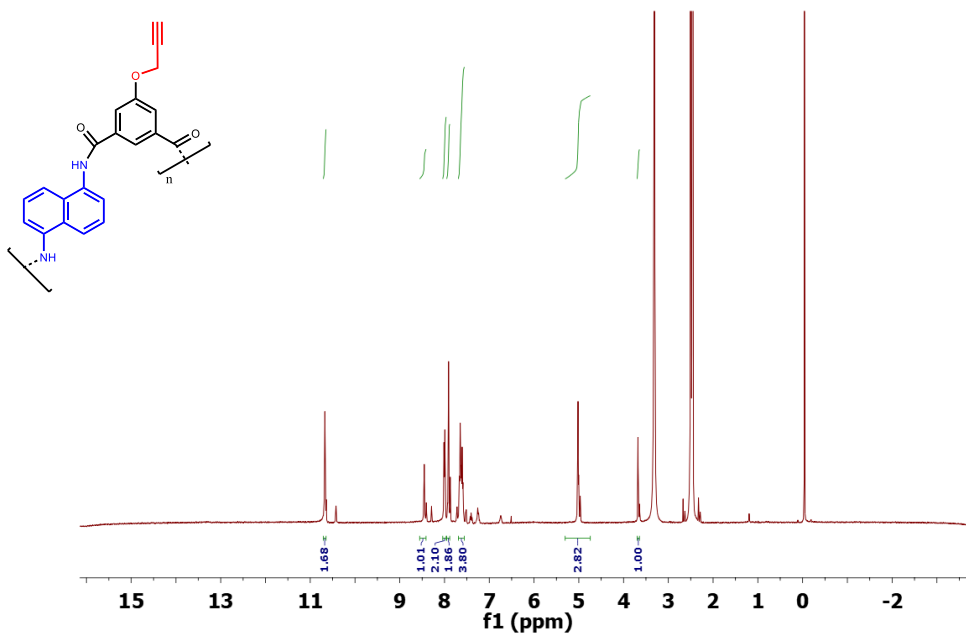
**Dimethyl 5-(prop2-yn-1-yloxy) isophthalate,  $^1\text{H}$  NMR (400 MHz,  $\text{CDCl}_3$ ):**



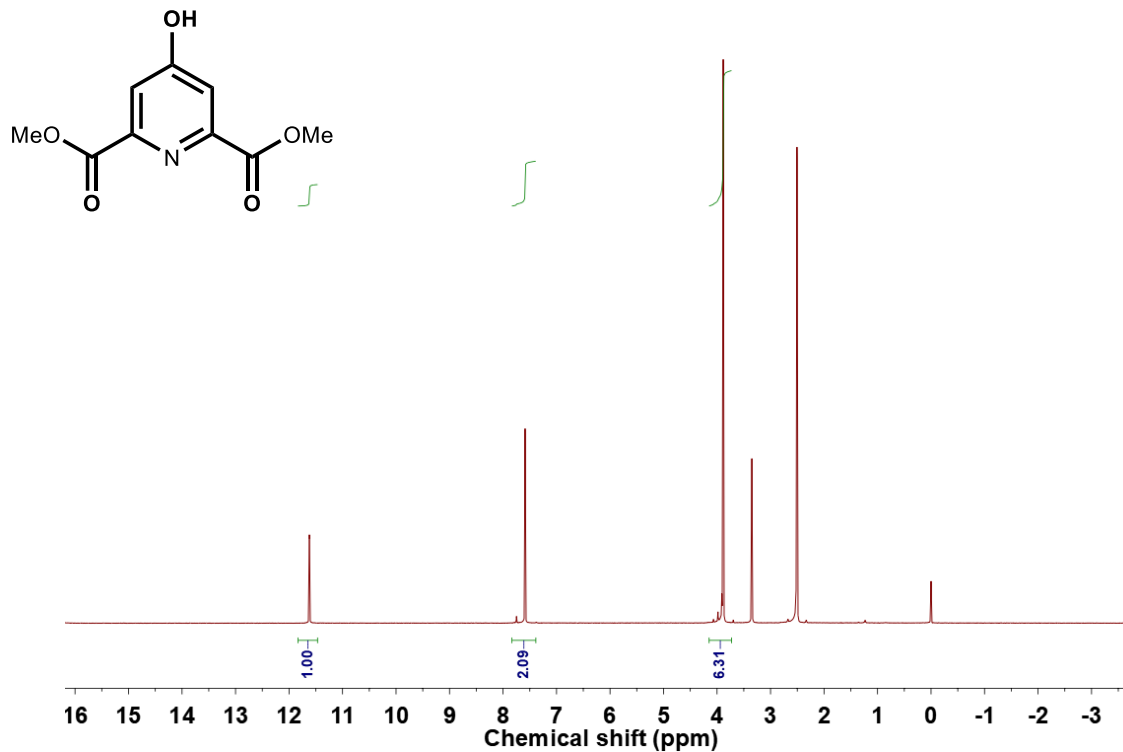
**5-(prop-2yn-1-yloxy) isophthalic acid,  $^1\text{H}$  NMR (400 MHz, DMSO):**



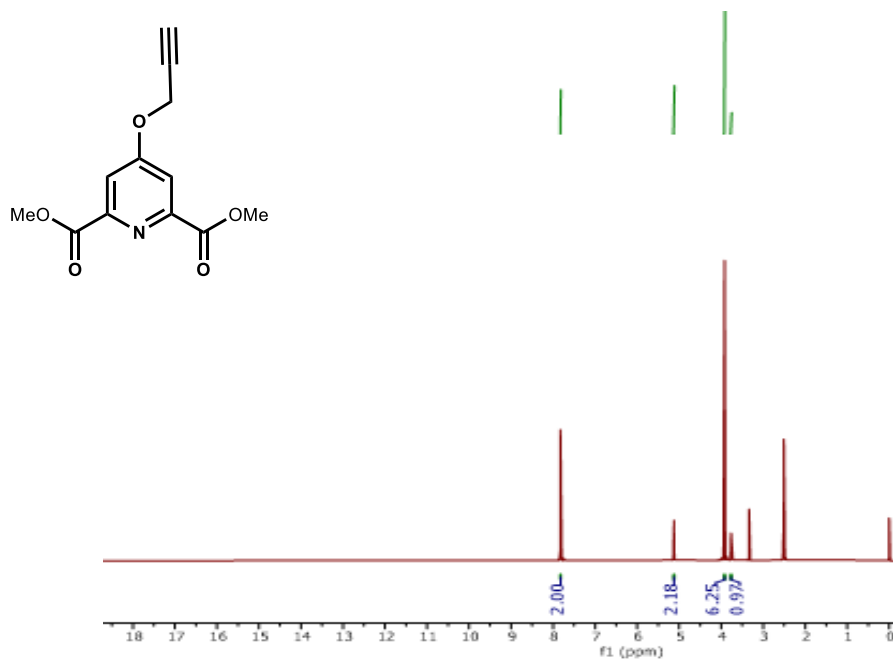
**POLY 10,  $^1\text{H}$  NMR (400MHz, DMSO):**



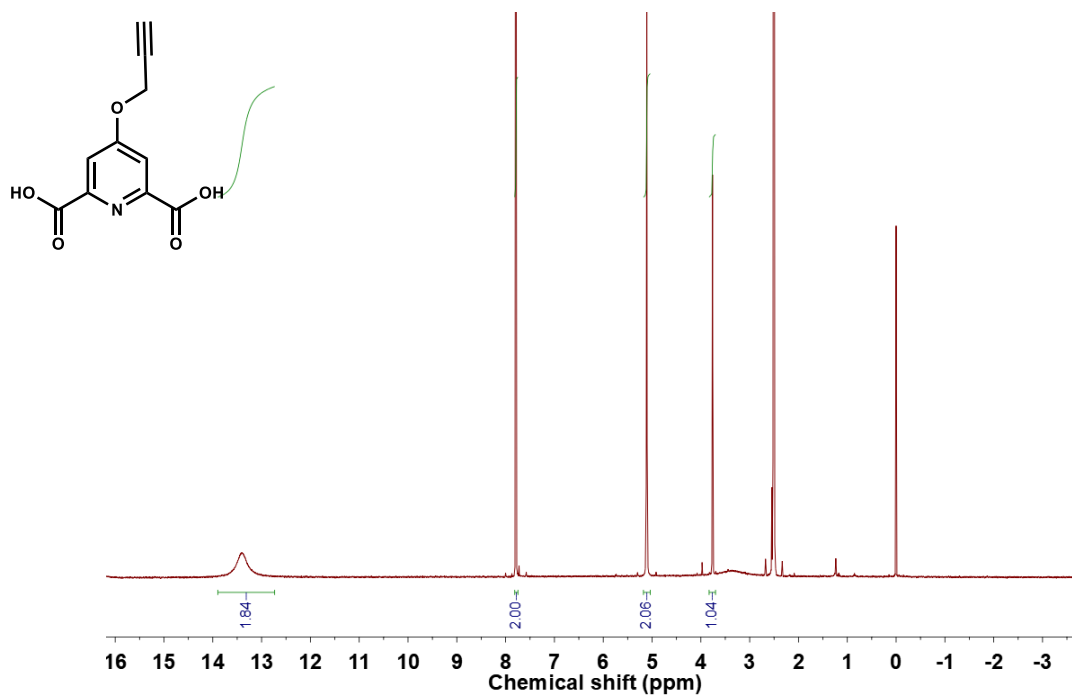
**Dimethyl 4-hydroxy pyridine-2, 6-dicarboxylate,  $^1\text{H}$  NMR (400MHz,  $\text{CDCl}_3$ ):**



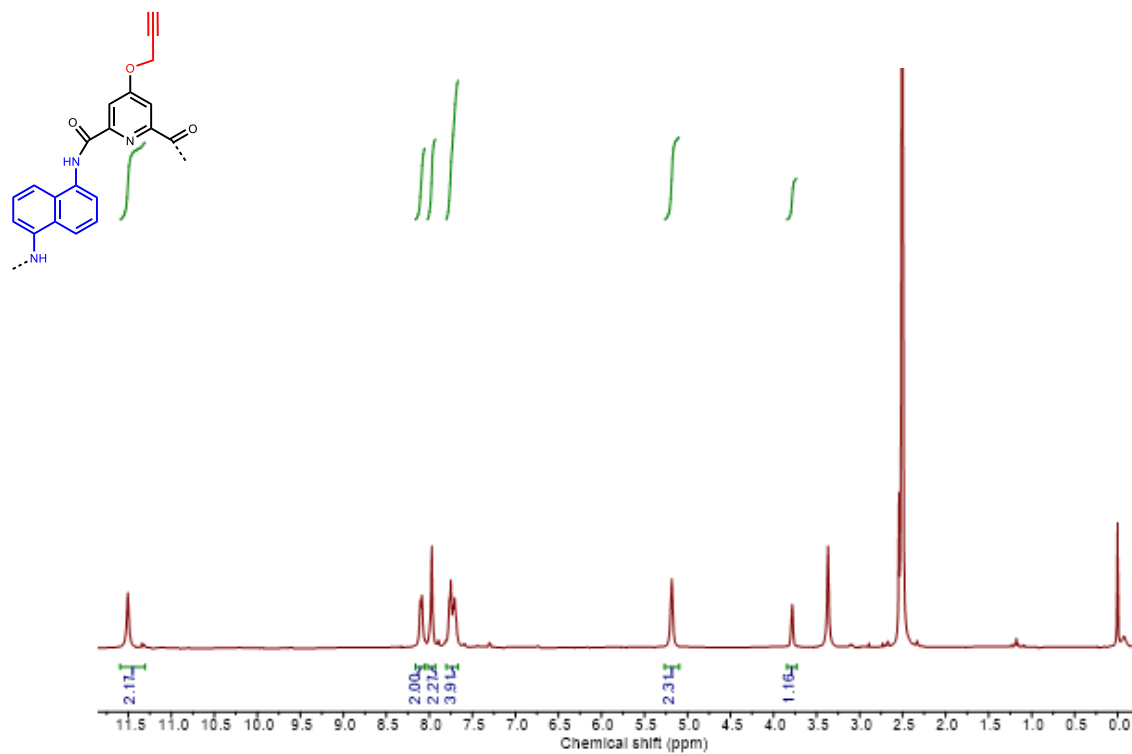
**Dimethyl 4-(prop-2-yn-1-yloxy) pyridine-2, 6-dicarboxylate ( $^1\text{H}$  NMR (400MHz,  $\text{CDCl}_3$ ):**



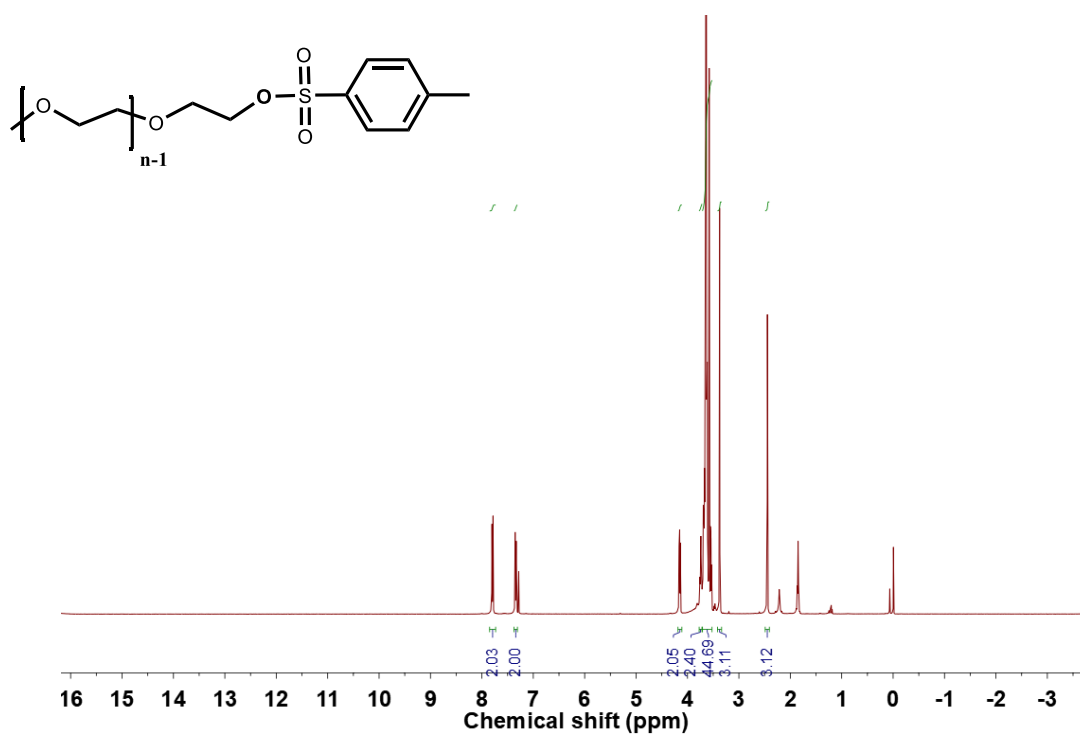
**4-(prop-2yn-1-yloxy) pyridine-2, 6-dicarboxylicacid ( $^1\text{H}$ NMR, 400MHz, DMSO):**



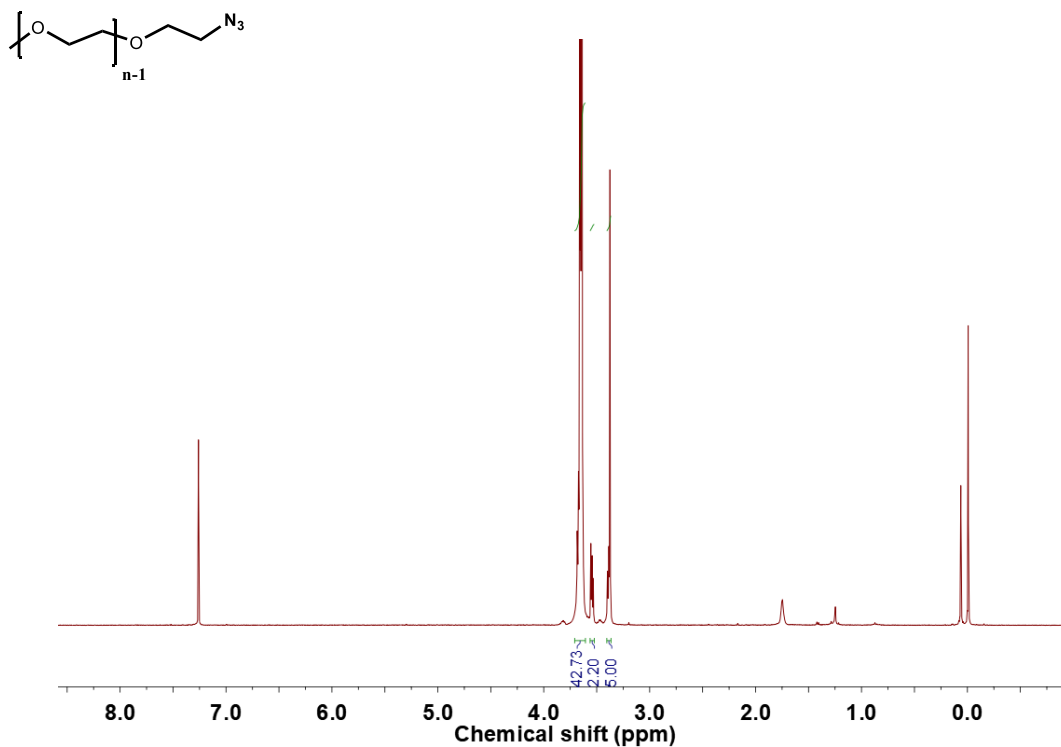
**POLY 11, 1H NMR (400MHz, DMSO):**



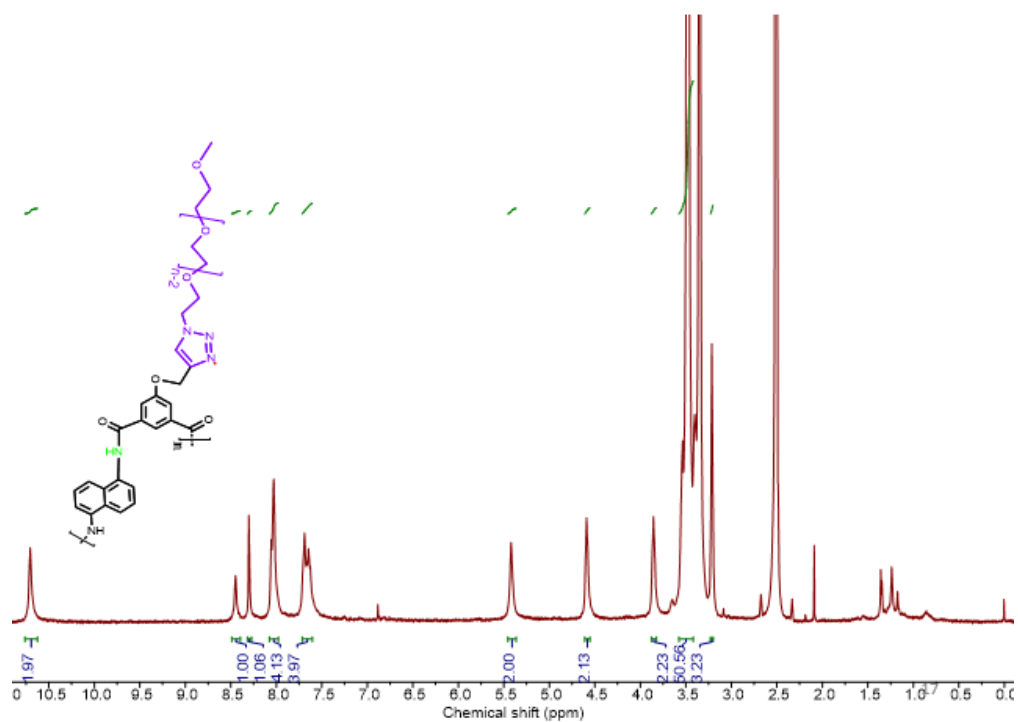
**PEG550-tosylate, <sup>1</sup>H NMR (400MHz, CDCl<sub>3</sub>):**



**PEG550-N<sub>3</sub>, <sup>1</sup>H NMR (400MHz, CDCl<sub>3</sub>):**



**POLY 10 (PEG550-N<sub>3</sub>), <sup>1</sup>H NMR (400MHz, DMSO):**



**POLY 11 (PEG550-N3), <sup>1</sup>H NMR (400MHz, DMSO):**

